

Suraj Gachhadar

Clock Error Impact on NB-IoT Radio Link Performance

School of Electrical Engineering

Thesis submitted for examination for the degree of Master of Science in
Communications Engineering.

Espoo 25.01.2018

Thesis Supervisor:

D.Sc. (Tech.) Kalle Ruttik

Author: Suraj Gachhadar		
Title: Clock Error Impact on NB-IoT Radio Link Performance		
Date: 25.01.2018	Language: English	Number of pages: 11+61
Department of Communications and Networking		
Professorship: Communications Engineering		code: ELEC3029
Supervisor: D.Sc. (Tech.) Kalle Ruttik		
<p>3GPP has recently addressed the improvements in Random Access Network (RAN) and specified some new technologies such as enhanced Machine Type Communication (eMTC) and Narrow Band – Internet of Things (NB-IoT) in its release 13 which is also known as LTE-Advanced Pro. These new technologies are addressed mainly to focus on development and deployment of cellular IoT services. NB-IoT is less complex and easily deployable through software upgradation and is compatible to legacy cellular networks such as GSM and 4G which makes it a suitable candidate for IoT. NB-IoT will greatly support LPWAN, thus, it can be deployed for Smart cities and other fields such as smart electricity, smart agriculture, smart health services and smart homes. The NB-IoT targets for low cost device, low power consumption, relaxed delay sensitivity and easy deployment which will greatly support above mentioned fields.</p> <p>This thesis work studies the clock error impact on the radio link performance for up-link transmission on the NB-IoT testbed based on Cloud-RAN using Software Defined Radios (SDR) on a LTE protocol stack. The external clock error is introduced to the network and performance issues are analyzed in the radio link. The analysis indicates packet drops up to 51% in the radio link through the study of received power, packet loss, retransmissions, BLER and SINR for different MCS index. The major performance issues depicted by the analysis are packet loss up to 51% and retransmission of packets up to 128 times for lower SINR and high clock errors. Also, clock errors produce CFO up to 1.25 ppm which results in bad synchronization between UE and eNodeB.</p>		
Keywords: 3 rd Generation Partnership Project (3GPP), Narrow Band-Internet of Things (NB-IoT), Clock Error, Block Error Rate (BLER), Modulation and Coding Scheme (MCS), Carrier Frequency Offset (CFO), Signal to Interference and Noise Ratio (SINR).		

Preface

This thesis was conducted in Department of Communications and Networking (COMNET), Aalto University. The thesis topic was interesting and I am grateful to work on it. I would like to thank to Viktor Nässi, resource manager at COMNET laboratory who provided all necessary equipments and support needed for the experiment. I would also like to thank Yihenew Beyene for helping and guiding me during the initial stage of the experiment.

Most of all, I would like to thank Kalle Ruttik for providing me this thesis topic, supervising my thesis, giving valuable feedbacks and comments and advising me throughout the thesis work.

Finally, I am grateful for the continuous support I received from my family and friends.

Espoo, 25.01.2018

Suraj Gachhadar

Contents

Table of Contents

Preface	iii
Contents	iv
Symbols and Abbreviations	vi
Symbols	viii
Tables and Figures	ix
1. Introduction	1
1.1 Objectives	2
1.2 Structure of the Thesis	2
2. Background	3
2.1 Narrow Band - Internet of Things (NB-IoT)	3
2.2 Narrow Band Downlink and Uplink Physical Channels	4
2.3 Performance issues on NB-IoT	5
2.4 OFDMA and SCFDMA Modulation in LTE and NB-IoT	8
2.5 Modulation and Coding Scheme (MCS)	10
2.6 Clock synchronization	11
2.7 Carrier Frequency Offset (CFO)	14
2.8 Carrier Synchronization Error	15
2.9 Phase Locked Loop (PLL) CFO Compensation Techniques	18
2.10 Sampling Clock offset (SCO)	20
2.11 Software Defined Radio (SDR)	22
3. Measurement System Description	26
3.1 Measurement Setup	26
3.2 Measurement Configuration	31
3.3 Measurement Data Processing	31
3.4 Issues during the measurement	32
4. Measurement Analysis	33
4.1 Change in Clock error to the change in Carrier Frequency Offset (CFO)	33
4.2 Analysis of Measurement Data	34
4.3 Analysis of Measurement Results	41

5. Discussions of Results	48
6. Conclusion.....	50
References	52
A Appendix: Modulation TBS index for PDSCH & PUSCH.....	55
B Appendix: Specifications of N2x0, Internal GPSDO and Rhode and Schwartz Signal Generator.....	57
C Appendix: Brief Introduction of the devices used for thesis work measurement	60
D Appendix: IP addresses of the USRPs and devices used in the measurement setup	60
E Appendix: Picture of the overall Measurement Setup.....	61

Symbols and Abbreviations

Abbreviations

3GPP	3rd Generation Partnership Project
ADC	Analog to Digital Converter
AWGN	Additive White Gaussian Noise
BLER	Block Error Rate
BPSK	Binary Phase Shift Keying
CAPEX	CAPital EXenditure
CDS	Channel Dependent Scheduling
CFO	Carrier Frequency Offset
CIR	Channel Impulse Response
CP	Cyclic Prefix
CQI	Channel Quality Indicator
CRC	Cyclic Redundancy Check
D2D	Device to Device
DAC	Digital to Analog Converter
DFT	Discrete Fourier Transform
DL	Download Link
eDRX	enhanced Discontinuous Reception
eMTC	enhanced Machine Type Communication
FFT	Fast Fourier Transform
FPGA	Field Programmable Gate Array
GNSS	Global Navigation Satellite System
GPS	Global Positioning System
GPSDO	GPS disciplined oscillator
GSM	Global System for Mobile Communications
HARQ	Hybrid Automatic Repeat Request
ICI	Inter Carrier Interference
IEEE	Institute of Electrical and Electronics Engineers
IoT	Internet of Things
LLC	Logical Link Control
LPWAN	Low Power Wide Area Network
LTE	Long Term Evolution
LTE MBMS	LTE- Multimedia Broadcast Multicast Service
LTE-A	LTE-Advanced
LTE-A eICIC	LTE-A enhanced Inter-Cell Interference Coordination
LTE-A MBSFN	LTE-A Multicast-Broadcast single-frequency network
LTE-FDD	LTE- Frequency Division Duplex
LTE-TDD	LTE- Time Division Duplex
M2M	Machine to Machine
MAC	Medium Access Control
MCL	Maximum Coupling Loss
MCS	Modulation and Coding Scheme

MIB	Master Information Block
MIMO/COMP	Multi Input Multiple Output/ Coordinated Multipoint
ML	Maximum Likelihood
MTC	Machine Type communication
NB-IoT	Narrow Band-Internet of Things
NBPBC	Narrowband Physical Broadcasting Channel
NCO	Numerically Controlled Oscillator
NPDCCH	Narrowband Physical Downlink Control Channel
NPDSCH	Narrowband Physical Downlink Shared Channel
NPRACH	Narrowband Physical Random Access Channel
NPSS	Narrowband Primary Synchronization Signal
NPUSCH	Narrowband Physical Uplink Shared Channel
NRS	Narrowband Reference Signal
NSSS	Narrowband Secondary Synchronization Signal
OCXO	Oscillator Controlled Crystal Oscillator
OFDM	Orthogonal Frequency Division Multiplexing
OFDMA	Orthogonal Frequency Division Multiple Access
OPEX	OPERational EXpenditure
PAPR	Peak to Average Power ratio
PLL	Phase Locked Loop
PPM	Parts Per Million
PPS	Pulse per Second
PRB	physical resource blocks
PTP	Precision Time Protocol
QAM	Quadrature Amplitude Modulation
QoS	Quality of Service
QPSK	Quadrature Phase Shift Keying
RAN	Random Access Network
RAR	Random Access Response
Rf	Radio frequency
RLC	Radio Link Control
SC	Sub Carrier
SCFDMA	Single Carrier Frequency Division Multiple Access
SCO	Sampling Clock Offset
SDR	Software Defined Radio
SINR	Signal to Interference and Noise Ratio
SNDCP	Sub Network Dependent Convergence Protocol
TBCC	Tail-Biting Convolutional Code
TBS	Transport Block Size
TCXO	Temperature-Compensated Crystal Oscillator
UE	User Equipment
UL	Upload Link
UMTS	Universal Mobile Telecommunications System
USRP	Universal Software Radio Peripheral
WCDMA	Wide Band Code Division Multiple Access

Symbols

f_1	Carrier frequency of transmitted signal
f_2	Carrier frequency of the received signal
$\delta f/\Delta f$	Carrier frequency offset
ϵ_I	Integral component
ϵ_f	Fractional component
f_s	Sub Carrier Spacing
θ	Phase shift
T	Symbol length, time between two consecutive OFDM symbols
T_{FFT}	FFT time; effective part of the OFDM symbol
k	Index of transmitted and received symbol
i	Index on Subcarrier
τ_{max}	Maximum excess delay of the channel
$n(t)$	Additive White Gaussian Noise (AWGN)
T_s	ideal sampling time
N	window interval
N_g	window with guard interval
δ	sampling clock offset

Tables and Figures

List of Table

Table 1. NB-IoT link budget for in-band deployment [6].....	6
Table 2. Latency Evaluation [8]	7
Table 3. 4 bit CQI table [10]	11
Table 4: Frequency and phase synchronization requirement for various cellular technologies, need of compliance and impact of non-compliance [10].....	13
Table 5. Clock errors and corresponding CFO for 640 MHz, 963 MHz and 1800 MHz.	33
Table 6. Statistics showing average retransmissions (R), number of packets decoded and SINR for different clock error and MCS index.....	35
Table 7. Statistics showing BLER and SINR for different clock error and MCS index.	38
Table 8. CFO, MCS and R (Avg.) at SINR \sim -5 dB	41
Table 9. CFO, MCS and BLER at SINR \sim -5 dB	45
Table 10. Modulation index and TBS index for PDSCH [10].....	55
Table 11. Modulation, TBS index and redundancy version for PUSCH [10]	56
Table 12. Specifications of USRP N2x0 from Ettus Research [28]	57
Table 13. Specifications of internal GPSDO kit from Ettus Research [29].....	58
Table 14. Specifications of Signal Generator from Rhode and Schwartz [30]....	59

List of Figures

Figure 1. NB-IoT stand-alone deployment and LTE in-band and guard band deployment.	3
Figure 2. Time multiplexing between NB-IoT downlink physical channels and signals.	4
Figure 3. OFDM signals (a) single carrier (b) Multiple carrier	8
Figure 4. Frame structure of OFDM signal.	9
Figure 5. SC-FDMA localized subcarrier mode and distributed mode [9].	10
Figure 6. OFDM signal with frequency offset δf causing ICI. The amplitude of the desired sub-carrier is reduced (“+”) and ICI arises from the adjacent sub-carrier (“O”).	15
Figure 7. OFDM baseband receiver architecture for CFO compensation using Phase locked loop (PLL) [15].	19
Figure 8. OFDM baseband receiver design using a frequency-domain interpolator to compensate the CFO [15].	19
Figure 9. (a) Sampling error due to sampling of transmitted signal $x(t)$ and received signal $z(t)$ at different clock rates. (b) Received signal $z(t)$ is expanded due to Doppler effect, resulting in sampling error even without clock rate mismatch.	20
Figure 10. Internal Architecture of USRP Device [16].	22
Figure 11. Time synchronous signal master-slave setup [21].	27
Figure 12. Digital oscilloscope Signals of master and slave at 10 MHz (scale: 200ns)	28
Figure 13. Spectrum analyzer showing master signal center frequency at 10 MHz	28

Figure 14. Overall setup for the measurement	30
Figure 15. Box plot showing distribution of R over SINR(γ) for clock error of 1 Hz.....	36
Figure 16. Box plot showing distribution of R over SINR(γ) for clock error of 12 Hz.....	36
Figure 17. (a) Plot showing SINR(γ) vs average retransmissions (R) for clock error of 1 Hz. (b) Plot showing SINR(γ) vs average retransmissions (R) for clock error of 12 Hz.	37
Figure 18. Plot showing SINR(γ) vs BLER for clock error of 1 Hz.....	39
Figure 19. Plot showing SINR(γ) vs BLER for clock error of 12 Hz.....	39
Figure 20. BLER ranging for 0 to 1. (a) SINR(γ) vs BLER plot for clock error of 1 Hz.....	40
(b) SINR(γ) vs BLER plot for clock error of 12 Hz.....	40
Figure 21. Plot showing SINR (γ) vs average retransmissions (R) for MCS 0. ..	42
Figure 22. Plot showing SINR (γ) vs average retransmissions (R) for MCS 3. ..	43
Figure 23. Plot showing SINR (γ) vs average retransmissions (R) for MCS 6. ..	44
Figure 24. Plot showing SINR (γ) vs BLER for MCS 0.	45
Figure 25. Plot showing SINR (γ) vs BLER for MCS 3.	46
Figure 26. Plot showing SINR (γ) vs BLER for MCS 6.	47

1. Introduction

The evolution of cellular technologies has made possible to connect everyone and everything around the world. The concept of connecting things is being implemented in large scale through the revolutionary concept known as Internet of things (IoT). The IoT aims to provide a platform for connecting massive number of devices and people together. There are billions of devices connected currently and Ericsson predicts that the connected devices will grow up to 28 billion by 2021 [2]. The enabling technologies for IoT that targets for reliable and massive connectivity such as Device to Device (D2D) communications and Machine Type communication (MTC) are already in the phase of research and implementation. There are several studies going on to combine cellular networks with IoT technologies to support massive connection of devices and people with more secure and reliable connection.

3GPP is collaborative group of telecommunication associations which is responsible to address the development and maintenance of cellular technologies. 3GPP proposes the upgrades and enhancements of technology through its release. There are several releases from 3GPP (Phase1, Phase2, ... Release 13) that proposes and plans for enhancements and developments of cellular networks and technologies. 3GPP introduced first IoT specific User Equipment (UE) in Release 12 (Rel-12) known as LTE-Cat0 or LTE-M, after which it has continued to enhance IoT enabling technologies from its upcoming releases. Recently, 3GPP Release 13 (Rel-13) addressed advancements in Random Access Network (RAN) and introduced new technologies such as enhanced MTC and NB-IoT (Narrow Band-Internet of Things) to support Cellular IoT. NB-IoT focuses on Low Power Wide Area Network (LPWAN) and its specifications are mainly addressed to target low cost of devices, low power consumption, long range and ease of deployment which makes it suitable candidate for IoT deployment. Besides NB-IoT, which is based on mobile network compatible to GSM and 4G, there are some other technologies such as LoRa and SIGFOX based on sub-GHZ spectrum that targets MTC and LPWAN. LoRa and SIGFOX uses unlicensed spectrum. The key difference between licensed and unlicensed spectrum based technologies is the quality of service (QoS) and interference related issues, that can be easily controlled in former case but it is difficult to manage in later case.

The deployment of new technologies is challenging and several complex or unexpected issues need to be addressed, analyzed and solved before commercializing it in large scale. Although, recently released NB-IoT has many useful and promising features such as 20dB enhanced link budget, low deployment cost and compatibility with legacy networks (4G and GSM) [1][2], it is vulnerable to issues such as network synchronizations and clock offsets. NB-IoT targets to achieve low cost of devices up to 5€ which hints the use of cheap oscillators that are poor in performance. The quality of clock oscillators found in the devices greatly affect the synchronization issue in the network. The mismatch of clock signal generated by the oscillators in UE and base stations introduce clock error. The clock error gives rise to Carrier Frequency offset (CFO) and sampling errors in the network and performance of radio link is greatly affected.

1.1 Objectives

The objective of this thesis is to measure the effect of clock error in the radio equipments (UE and eNodeB) of NB-IoT and analyze performance of the radio link due to clock error. The similar observation has been performed earlier in [8] using internal clock oscillator of USRPs (Universal Software Radio Peripheral). The motivation for this work is to find out the sensitivity of the NB-IoT system performance towards clock errors. For this purpose, external clock signal is fed to the URSP devices. The clock errors are introduced in the system in a controlled manner to see the impact of clock errors.

The thesis work measures and analyzes uplink signal informations, where UE and eNodeB are fed with external clock signal. The NB-IoT system, that is implemented on Software Defined Radio (SDR) based C-RAN testbed [8] is fed with external clock signal and measurements are collected for analysis at various SINR and clock errors. The uplink transmission of packets is configured in the system. The impact of clock error on performance of radio link has been measured for which data analysis is performed for important parameters such as received power (P_r), Signal to Interference and Noise Ratio (SINR), retransmissions (R), and Block Error Rate (BLER) for three different Modulation and Coding scheme (MCS) Index. The parameters above reflect quality and strength of a signal. Therefore, their analysis provides critical information about the radio link performance. The performance impact is illustrated in chapter 4, which shows effect of clock error in the system. Further, the clock error in the system leads to carrier frequency offset (CFO). The change in clock error to the change in CFO is also studied in this thesis.

1.2 Structure of the Thesis

The thesis work is split into 6 chapters. Chapter 2 introduces the background materials related to the NB-IoT and its performance issues, modulation schemes, MCS index, clock synchronization and CFO. Chapter 3 describes setup and implementation of the measurement system. Similarly, chapter 4 focuses on evaluation and analysis of measured data. Chapter 5 discusses the result of this thesis work and Chapter 6 summarizes the thesis work and talks about further research towards analysis of clock error impact.

2. Background

2.1 Narrow Band - Internet of Things (NB-IoT)

NB-IoT is a new technology introduced by 3rd Generation Partnership Project (3GPP) in its Release 13 which is also known as LTE Advanced Pro. LTE Advanced Pro also introduces other new technology called eMTC (enhanced Machine Type Communication, often referred as LTE-M). These technologies are introduced mainly to support IoT in future. NB-IoT aims to address the requirements of IoT such as lower device cost (up to 5€ [1][2][3]), long battery life (up to 10 years [1][2][3]), extended coverage (link budget enhancement by 15-20 dB [1]), lower deployment cost (minimum CAPEX and OPEX through software upgrade [1]) and massive number of device support (up to 50,000 connections per cell [3]). Further, it aims to work with both cellular (licensed spectrum) and non-cellular (unlicensed spectrum) IoT.

NB-IoT is specifically developed technology to support massive IoT deployment. It is simple and has minimum features to reduce complexity. Several advanced and even basic features of LTE-A such as carrier aggregation, lack of handover in UEs in the connected state, dual connectivity, or device-to-device services are not supported in NB-IoT. Moreover, cell reselection is restricted in it. Therefore, NB-IoT technology is an approach to support services and applications that are non-delay sensitive, can work with higher latency and requires minimum Quality of Service (QoS) [4].

NB-IoT is typically developed to work in lower spectrum (less than 1 GHz) to achieve maximum coverage and it occupies a bandwidth of only 180 KHz, which provides it a deployment flexibility. NB-IoT carrier can possibly be deployed as standalone carrier in GSM band, in-band and guard band carrier in LTE band. The standalone carrier deployment utilizes the new bandwidth of 200KHz available in GSM band, guard-band carrier uses the reserved guard band bandwidth of LTE band, whereas, in-band carrier uses or shares the same resource block of LTE carrier [3].

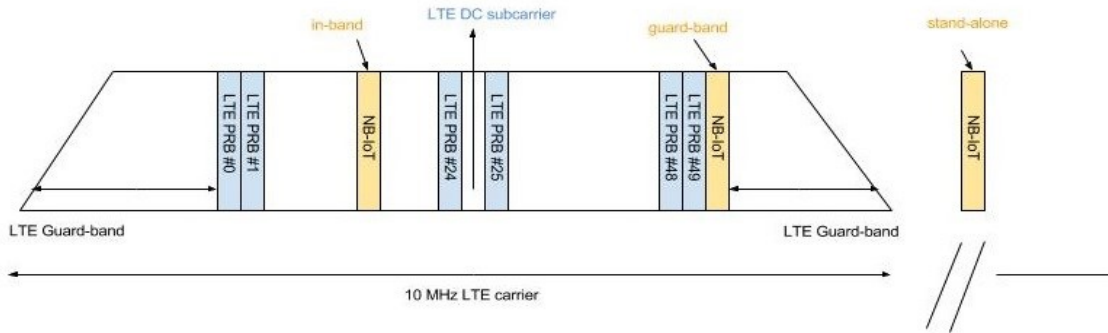


Figure 1. NB-IoT stand-alone deployment and LTE in-band and guard band deployment.

The features of this new technology other than discussed above are use of FDD half-duplex type-B duplex mode, increased UE transmit power of 23 dBm, data rate (instantaneous peak rates) of up to 170 Kbps for downlink and 250 Kbps for uplink and 20 dB additional link budget [1].

2.2 Narrow Band Downlink and Uplink Physical Channels

NB-IoT defines downlink channels and signals in following manner.

- Narrowband Primary Synchronization Signal (NPSS) - It is used for performing cell search which includes time and frequency synchronization and cell identity detection. It is transmitted in sub frame #5 in every 10ms frame using the last 11 OFDM carriers in the sub frame [5].
- Narrowband Secondary Synchronization Signal (NSSS) - It has similar function as NPSS such as cell identity group detection and it is transmitted in sub frame #9 also using the last 11 OFDM symbol in the sub frame and it has 20ms periodicity [5].
- Narrowband Physical Broadcasting Channel (NPBCH) - It carries the master information block (MIB) and is transmitted in sub frame #0 in every 10ms frame [5].
- Narrowband Physical Downlink Control Channel (NPDCCH) - It carries scheduling information for both uplink and downlink data channels. It also carries the HARQ acknowledgement information for the uplink data channels as well as paging indication and random access response (RAR) scheduling information [5].
- Narrowband Physical Downlink Shared Channel (NPDSCH) - It carries data from higher layers and paging message, system information, and the RAR message. The maximum transport block size of NPDSCH is 680 bits. NPDSCH and NPDCCH are allocated various sub frames to carry information [5].
- Narrowband Reference Signal (NRS) - It is used to provide reference for the demodulation of the downlink channels [5].

All the downlink channels use the LTE tail-biting convolutional code (TBCC) to reduce the complexity of UE.

Even numbered frame	Subframe number									
	0	1	2	3	4	5	6	7	8	9
	NPBCH	NPDCCH Or NPDSCH	NPDCCH Or NPDSCH	NPDCCH Or NPDSCH	NPDCCH Or NPDSCH	NPSS	NPDCCH Or NPDSCH	NPDCCH Or NPDSCH	NPDCCH Or NPDSCH	NSSS
Odd numbered frames	Subframe number									
	0	1	2	3	4	5	6	7	8	9
	NPBCH	NPDCCH Or NPDSCH	NPDCCH Or NPDSCH	NPDCCH Or NPDSCH	NPDCCH Or NPDSCH	NPSS	NPDCCH Or NPDSCH	NPDCCH Or NPDSCH	NPDCCH Or NPDSCH	NPDCCH Or NPDSCH

Figure 2. Time multiplexing between NB-IoT downlink physical channels and signals.

The uplink channels are defined as follows:

- Narrowband Physical Random Access Channel (NPRACH) - It has been newly designed for NB-IoT as legacy LTE uses bandwidth of 1.08 MHz which is higher than total bandwidth of NB-IoT i.e. 180 KHz. The preamble of NPRACH consists of 4 symbol groups, each symbol group having one CP and 5 symbols. The CP length varies according to format 0 and format 1 which corresponds to 66.67us for 10km of cell radius and 266.7us for cell radius up to 40km. The waveform of NPRACH is referred to as frequency hopping and to support coverage extension, the preamble can be repeated 128 times.
- Narrowband Physical Uplink Shared Channel (NPUSCH) - It has two formats: Format 1 and Format 2. The former is used for carrying uplink data and maximum TBS is 1K bits. It supports multi-tone transmission as legacy LTE and can allocate 12, 6, or 3 tones. The latter is used for signaling HARQ acknowledgement for NPDSCH and uses a repetition code for error correction. NPUSCH supports single-tone transmission based on 15 KHz and 3.75 KHz carrier spacing, which uses $\pi/2$ -BPSK or $\pi/4$ -QPSK with phase continuity between symbols to reduce PAPR [5][6][7].

2.3 Performance issues on NB-IoT

NB-IoT targets to support low cost device, long battery life of devices, extended coverage and low deployment cost of the network and delay tolerant services and applications. The targets can be achieved through several extensions and modifications added to LTE in Release 13 (Rel. 13) by 3GPP. There have been several studies on performance analysis of NB-IoT assuming various parameters and system deployments. The overview of such analysis is described in brief in this chapter.

A. Long Battery Life

The battery life of devices is aimed up to 10 years and more at Maximum coverage level with Maximum Coupling Loss (MCL) of 164 and battery capacity of 5 watts. The studies have shown that the long battery life is possible because of the long eDRX (enhanced Discontinuous Reception) and power saving mode (PSM) [6]. eDRX allows UE to sleep up to 1000 seconds while waking up periodically to check for paging while in PSM the UE is in power off or sleep mode, registered to but not reachable by the network. Further, the studies show that estimated battery life of 10.5 years and 16.8 years can be achieved if 200 bytes and 50 bytes is exchanged daily between UE and eNodeB [6].

B. Extended coverage

NB-IoT goal is to achieve MCL of 164 dB by enhancing sensitivity by 20 dB, thus improving the cell coverage. The link budget for NB-IoT in stand-alone and in-band mode from several studies shows that MCL of 164 dB is achievable for the channels considered using Rel. 13 features. In in-band deployment, 46 dBm power is available at eNodeB in downlink for LTE

and NB-IoT, out of which 35 dBm is used for NB-IoT (corresponding to 6 dB power boosting of baseline). The downlink and uplink data rate in application layer is 0.40 kbps and 0.27 kbps. The link budget for in-band deployment is shown below [6].

Table 1. NB-IoT link budget for in-band deployment [6]

Channel	NPBCH	NPDCCH	NPDSCH	NPRACH	NPUSCH	
Transport block size (bits)			256		696	696
Number of resource units			10		10	10
Transmission time (ms)			640		2560	2560
Subcarrier spacing (KHz)	15	15	15	3.75	15	3.75
No of subcarrier	12	12	12	1	1	1
Max Tx power (dBm)	46	46	46	23	23	23
Actual Tx power (dBm)	35	35	35	23	23	23
Thermal noise density (dBm/Hz)	-174	-174	-174	-174	-174	-174
Receiver noise figure (dB)	5	5	5	3	3	3
Interference margin (dB)	0	0	0	0	0	0
Occupied channel BW (Hz)	180,000	180,000	180,000	3,750	15,000	3,750
Effective noise power (dBm)	-116.4	-116.4	-116.4	-135.3	-129.2	-135.3
Required SINR (dB)	-12.6	-13.0	-12.8	-5.8	-11.9	-5.5
Receiver sensitivity (dBm)	-129.0	-129.4	-130.1	-141.1	-141.1	-140.8
MCL (dB)	164.0	164.4	164.3	164.1	164.1	163.8

C. Low device cost

The main factor for cost of devices is complexity of the network. The complexity of the systems increases as their performance is optimized. 3GPP recent releases, Rel. 12 and Rel.13 have introduced a lower complexity and simpler device categories to support IoT and M2M. The lower data rates of 170 kbps (DL) and 250 kbps (UL), half duplex mode, bandwidth of 180 KHz, 1 antenna UE features in NB-IoT has greatly reduced the complexity and cost of the devices and it is possible to produce devices less than 5€. Further, the lower power device of 20/23 dBm allows integration of power amplifiers in a single chip and mass production of it highly reduces the device cost [1].

D. Capacity

The NB-IoT aims to connect massive number of devices and the target is to support nearly 52000 devices within a cell-site. The studies show that a cell-site sector per NB-IoT carrier can support

250,000 devices and additional devices can supported through multiple carrier. The studies are based on traditional macro system simulation with 19-site, 57-cell system setup with wrap around interference allocation [6][7].

E. Latency

The target of NB-IoT is to support services that are non-delay sensitive and can tolerate latency of up to 10 seconds. The analysis from studies shows that latency of 9.9 seconds can be achieved with 99.9% confidence. The latency report is assumed to consist 20 bytes application report, 65 bytes upper layer protocol header and 15 bytes of SNDCP/LLC/RLC/MAC/CRC overhead [8]. The below table shows the time used in calculating the latency which includes synchronization, master information block acquisition, random access (including wait time), uplink scheduling grant and data transmission targeting 99% confidence level [6].

Table 2. Latency Evaluation [8]

Activity	Stand-alone	In-band
Synchronization	520	1110
MIB acquisition	640	1920
PRACH	1440	1440
Wait	572	1440
DCI + RAR	72	288
Msg3	349	349
DCI + Msg4	83	299
DCI (UL grant)	45	153
UL Data Tx (99% confidence)	2883	2883
Total Latency	6604	9882

F. Low deployment cost

The reuse of existing network (LTE and GSM) can greatly reduce the deployment cost of NB-IoT network. Further, the simple software upgradation on the existing LTE network without the need of reinstalling hardware will reduce the deployment cost of NB-IoT network with higher coverage than existing LTE network [1]. The LTE network and NB-IoT can use the same hardware and share spectrum without running into coexistence problems because of is different deployment modes (in-band, guard-band and stand-alone) [1].

2.4 OFDMA and SCFDMA Modulation in LTE and NB-IoT

The physical layer for NB-IoT inherits features from legacy LTE OFDMA downlink with subcarrier spacing of 15 KHz. There are 12 subcarriers for a bandwidth of 180 KHz in case of NB-IoT which is equal to one Physical Resource Block (PRB) of LTE. This makes NB-IoT compatible with LTE OFDMA symbol structures and both technologies can coexist together. Further, frame, sub frame and slot duration of 10ms, 1ms and 0.5ms is identical to legacy LTE. Slot format in terms of cyclic prefix (CP) and number of OFDMA symbols per slot is also identical to LTE.

The uplink transmission supports SCFDMA with subcarrier spacing of 15 KHz and 3.75 KHz with single-tone and multi-tone transmission. The single-tone supports both 15 KHz and 3.75 KHz. 15 KHz transmission being inherited from LTE with same slot and sub frame time of 0.5ms and 1 ms while 3.75 KHz uses 2ms slot duration. The multi-tone uses only 15 KHz subcarrier spacing having same block format as LTE. The orthogonality between subcarrier is maintained in 15 KHz subcarrier spacing which makes NB-IoT best for coexistence with LTE. In 3.75 KHz subcarrier spacing, the orthogonality is bit difficult to achieve. The bandwidth of the channel is 180 KHz, which is same as downlink and the number of subcarriers for 15 KHz and 3.75 KHz spacing is 12 and 48.

Orthogonal Frequency Division Multiplexing (OFDM) is a multicarrier modulation, which divides the available bandwidth into many subcarriers and transmits the data in each of the subcarrier. The subcarriers maintain orthogonality between each other thus eliminating inter-carrier interference (ICI). The data is transmitted over each subcarrier in parallel stream with each subcarrier being modulated separately using various level of modulation (i.e. QPSK, QAM, 64QAM) depending on signal quality. Therefore, each OFDM symbol is the linear combination of instantaneous signal on each of the subcarrier in the channel.

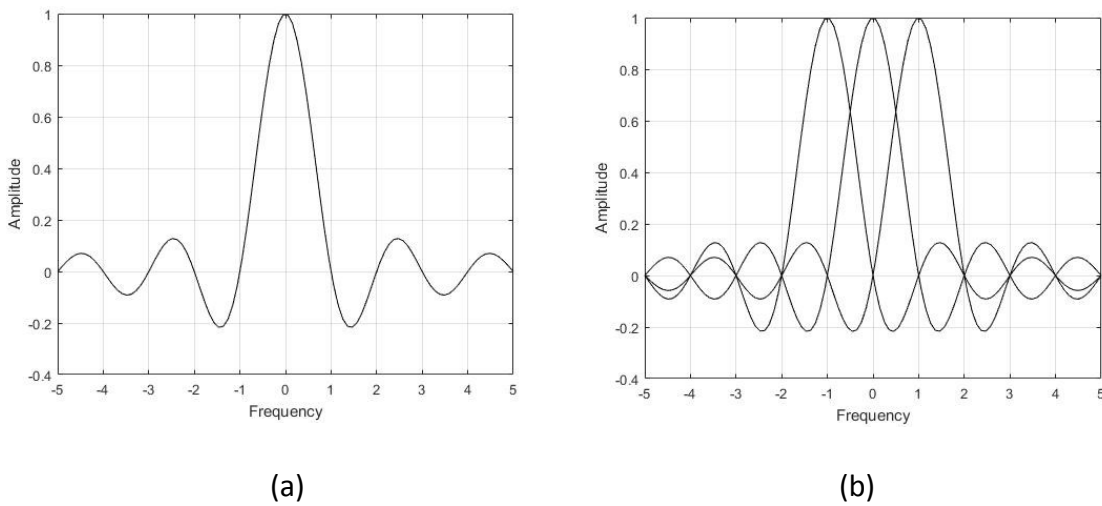


Figure 3. OFDM signals (a) single carrier (b) Multiple carrier

The OFDM symbols consists of two major components, cyclic prefix (CP) and data where CP is used to eliminate inter symbol interference (ISI). Further, OFDM subcarriers are closely spaced to make efficient use of available bandwidth which increases the spectral efficiency of the system.

The multiple access technique used in downlink in legacy LTE and NB-IoT is OFDMA. The users are allocated a specific number of subcarriers (PRB) for a predetermined amount of time. PRB has both time and frequency dimensions and allocation of PRB is determined by base station (eNodeB) of LTE. Each resource block has a bandwidth of 180 KHz and there are 12 subcarriers with spacing of 15 KHz. The number of available PRB's varies according to the bandwidth of the LTE spectrum. The generic frame structure of LTE has a period of 10ms. The frame consists of sub-frames with duration of 1ms and each sub-frame is divided into two slots of 0.5ms. Slots consist of either 6 or 7 OFDM symbols depending on whether normal or extended CP is applied. A PRB consists of 12 consecutive subcarriers for one slot (0.5ms) and it is the smallest unit assigned by the base station.

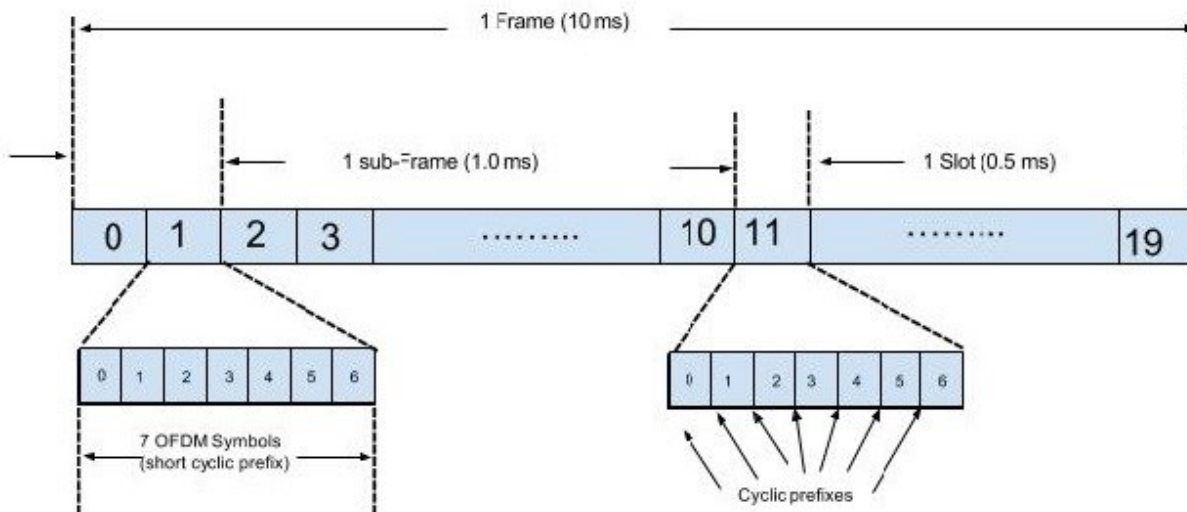


Figure 4. Frame structure of OFDM signal.

There are several advantages of OFDM over single carrier modulation such as high spectral efficiency, robust against ISI and fading channels. This makes OFDMA a good access technique for LTE. However, OFDM suffers from high peak to average power ratio (PAPR) and it is susceptible to carrier frequency errors due to local oscillators and Doppler effects.

OFDMA is widely used in downlink of LTE because of its advantages. The high PAPR of OFDM makes it however a bad choice for uplink since the requirements of uplink varies in several ways from downlink. The power consumption is one of the main issue for UE terminals

and with high PAPR and loss of efficiency, OFDM is replaced by an alternative access technique called SC-FDMA.

SC-FDMA is widely adopted for LTE and E-UTRA for the uplink transmission because of low PAPR and reduced cost of power amplifier. SC-FDMA transmission is similar to that of OFDMA, where data is transmitted over the air interface in many subcarriers. The orthogonality of the subcarriers is maintained by the addition of the cyclic prefix. In SC-FDMA, the information of each bits is spread over all the subcarrier with the use of an additional DFT block before the subcarrier mapping. The subcarriers are thus set of non-overlapping Fourier coefficients. This leads to a single-carrier transmit signal that distinguishes SC-FDMA from OFDMA, which is a multi-carrier transmission scheme. The subcarriers are not modulated individually in SC-FDMA, which results in low PAPR than OFDMA.

SC-FDMA has similar generic frame structure as OFDMA with frame, sub-frame and slot duration of 10ms, 1ms and 0.5ms with CP preceded in the SC-FDMA symbols. The SC-FDMA subcarrier mapping can be classified in two ways, localized mode and distributed mode. In localized mode, the assigned discrete subcarriers are mapped consecutively confined to fraction of total bandwidth whereas in distributed mode, the subcarriers are mapped non-consecutively over the entire bandwidth. The localized mode is preferred over distributed mode in LTE uplink transmission because of its higher performance and possibility to exploit frequency selective gain via channel dependent scheduling (CDS) [9].

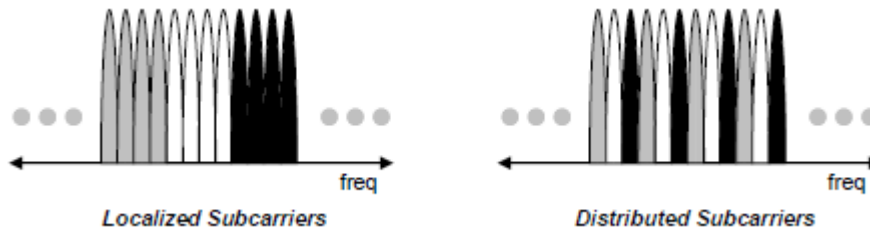


Figure 5. SC-FDMA localized subcarrier mode and distributed mode [9]

2.5 Modulation and Coding Scheme (MCS)

MCS index value describes modulation types and coding rate that is applied in a channel. The MCS is a combination of number of spatial streams + modulation type + coding rate. The spatial streams can range from 1 to 4, resulting higher throughput for larger value. The modulation type can be QPSK, 16-QAM and 64-QAM as defined in the MCS index value. The coding rate can be $\frac{1}{2}$, $\frac{3}{4}$, $\frac{5}{6}$ corresponding to that one redundancy bit is inserted for every single, third and fifth bits of data. The higher MCS value indicates higher data rate and more bits per symbol. The MCS index are standardized by the IEEE and 3GPP for various technologies during their release. The Table 3 below shows 4-bit Channel Quality Indicator (CQI) from the 3GPP release 8. The modulation and TBS index table for PDSCH and PUSCH can be found in appendix A.

Table 3. 4 bit CQI table [10]

CQI index	modulation	code rate * 1024	efficiency
0	out of range		
1	QPSK	78	0.1523
2	QPSK	120	0.2344
3	QPSK	193	0.3770
4	QPSK	308	0.6019
5	QPSK	449	0.8770
6	QPSK	602	1.1758
7	16QAM	378	1.4766
8	16QAM	490	1.9141
9	16QAM	616	2.4063
10	64QAM	466	2.7305
11	64QAM	567	3.3223
12	64QAM	666	3.9023
13	64QAM	772	4.5234
14	64QAM	873	5.1152
15	64QAM	948	5.5547

2.6 Clock synchronization

All devices in a network (wired or wireless) needs to be clock synchronized for better functioning of the network. Every device in a network has their own clock oscillator and each clock has its own offset and drift. It is important in a network to implement a proper channel and protocol to keep all device synchronized in time. The devices should have proper communication between each other and with the central station (base station) to keep themselves aware of the clock offset and maintain it accordingly to maintain synchronization. Synchronization in telecommunications networks is the process of aligning the time scales of transmission and switching equipment so equipment operations occur at the correct time and in the correct order. Synchronization requires the receiver clock to acquire and track the periodic timing information in a transmitted signal.

Poor synchronization in digital networks can lead to problems such as:

- Block retransmission
- Deletion or repetition of data
- Loss of voice or data transmission
- High Energy consumption of UE as it tries to synchronize with eNodeB
- Partial or complete traffic stoppage

Synchronization of signal can be performed with respect to frequency, phase and time. Frequency synchronization is achieved easily as there are many systems and devices to produce nearly identical frequencies. Phase and time synchronization requires high accuracy and stability which makes them difficult to achieve and makes system complicated. The synchronization techniques are briefly explained below.

Frequency synchronization

It is a process where two clock signal pulse are aligned in terms of repeating interval in frequency but not in terms of phase or time.

In NB-IoT testbed used in this thesis, clock signals synchronization is achieved by two sinusoidal signal having same frequency.

Phase synchronization

Two clock signals are aligned in terms of repeating interval in frequency and phase (one second interval) but without a common time of origin.

Time synchronization

The clock signals have common time origin and they are frequency and phase synchronized.

Time synchronization can partly be related to frame synchronization of two OFDM signals in our system (NB-IoT testbed). OFDM frames are aligned from the same starting moment common time origin).

The synchronized signal becomes more precise and accurate when it is synchronized in frequency, phase and time.

Depending on various technologies and applications, the synchronization precision varies. The below table shows the synchronization requirement for various technologies, why synchronization is needed and the effect of not meeting the synchronization.

Table 4: Frequency and phase synchronization requirement for various cellular technologies, need of compliance and impact of non-compliance [10].

Technologies	Frequency Network/ Air interface	Phase	Need for compliance	Impact or effect of non- compliance
GSM, UMTS, WCDMA	16 ppb/ 50 ppb	---	-----	----
CDMA2000	16 ppb/ 50 ppb	$\pm 3.5\mu s$ to $\pm 10\mu s$	-----	-----
LTE-FDD	16 ppb / 50 ppb	----	Call initiation	Call inter- ference and dropped calls
LTE-TDD	16 ppb / 50 ppb	$\pm 1.5\mu s$ (<3km cell radius) $\pm 5\mu s$ (>3kmcellradius)	Time slot alignment	Packet loss /co- llisions and spectral inefficiency
LTE MBMS (LTE-FDD and LTE-	16 ppb / 50 ppb	$\pm 10\mu s$ (inter- cell time	----	-----
LTE-Advanced(LTE-A)	16 ppb / 50 ppb	$\pm 1.5\mu s$ to $\pm 5\mu s$	----	----
LTE-A MBSFN	16 ppb / 50 ppb	$\pm 1.5\mu s$ to $\pm 5\mu s$	Proper time alignment of video signal decoding from multiple BTSs	Video broad- cast interrupt
LTE-A MIMO/COMP	16 ppb / 50 ppb	$\pm 1.5\mu s$ to $\pm 5\mu s$	Coordination of signals to/from multiple BS	Poor signal quality at edge of cells, LBS accuracy
LTE-A eICIC	16 ppb / 50 ppb	$\pm 1.5\mu s$ to $\pm 5\mu s$	Interference coordination	Spectral inefficiency and service

It is understood from above table that synchronization is needed for more reliable and efficient network and services. The unsynchronized networks and devices can lead to various undesirable effects such as packet drops, call interference, spectral inefficiencies and poor signal quality. The new cellular technologies are getting more advanced and so does it network complexity

with the need of highly synchronized network signal to fulfill the demands of end user customers with new applications and services.

The mobile cellular technologies such as 2G, 3G and LTE-FDD requires only frequency synchronization with accuracy within 50 ppb at the radio interface [10]. The latest and advanced cellular technologies such as LTE-TDD and LTE-A has added phase and time synchronization requirement as well, which is difficult to acquire. There are several synchronization methods to achieve nearly perfect synchronization in the mobile networks such as GNSS everywhere, PTP with boundary clock and PTP profile with full on/path support. These topics are not discussed in detail as they are out of scope of this thesis. The network synchronization in a mobile system is a huge topic itself and requires a thorough learning and understanding while this thesis only tries to get the basics of clock synchronization in a small network.

2.7 Carrier Frequency Offset (CFO)

Carrier Frequency offset (CFO) is the difference between transmitter and receiver local oscillator frequency. The transmitters and receivers have their own local oscillators and they never oscillate at identical frequency. This results in two peak carrier frequencies, one of which is not the original signal transmitted. This can lead to inter carrier interference (ICI) in OFDM system and destroy the orthogonality of carrier signals and also degrade the bit error rate (BER). Further, CFO is also produced when transmitter or receiver is moving which is known as Doppler Effect. Generally, the effect of oscillator mismatch in CFO is higher than the Doppler Effect.

The complex baseband equivalent model of the transmitted signal is $x_t(t) = x(t)e^{j2\pi f_1 t}$, where $x(t)$ is time variant, multipath fading channel and f_1 is the carrier frequency of transmitted signal. At receiver, the received signal can have different carrier frequency f_2 due to mismatch of the local oscillator frequency of transmitter and receiver. The mathematical expression of the received signal is $r_t(t) = r(t)e^{j2\pi f_2 t}$, where $r(t)$ is time invariant multipath fading channel and f_2 is the carrier frequency of received signal. The carrier frequency offset δf is therefore the difference between carrier frequency of transmitted and received signal, $[\delta f = f_2 - f_1]$.

In a standard-compliant communication system, such as IEEE 802.11 the oscillators have tolerance values of around ± 20 ppm to produce as much identical frequency as possible. The CFO produced can be -40ppm to 40ppm. For example, if a transmitter oscillator is oscillating at 20ppm above nominal frequency and receiver oscillator is oscillating at 20ppm below, then the CFO is 40ppm. With 2.4 GHz, the CFO is ± 96 KHz. It is often preferred to denote high frequency errors in parts per million (ppm) or parts per billion (ppb) rather than in Hz. Error in Hz can be converted to ppm $\frac{(\text{error frequency}) * 10^6}{(\text{clock frequency})}$.

2.8 Carrier Synchronization Error

OFDM signal suffers from frequency offset which is typically introduced by frequency mismatch in the local oscillator of transmitter and receiver. The offset is also produced by the Doppler Effect when the transmitter or receiver is moving. The offset caused by the carrier synchronization error gives rise to Inter Carrier Interference in OFDM.

The impact of a frequency error can be seen as an error in the frequency instances, where the received signal is sampled during the demodulation by the FFT. Figure 6 depicts this two fold effect. The amplitude of the desired SC is reduced (“+”), and ICI arises from the adjacent SCs (“O”).

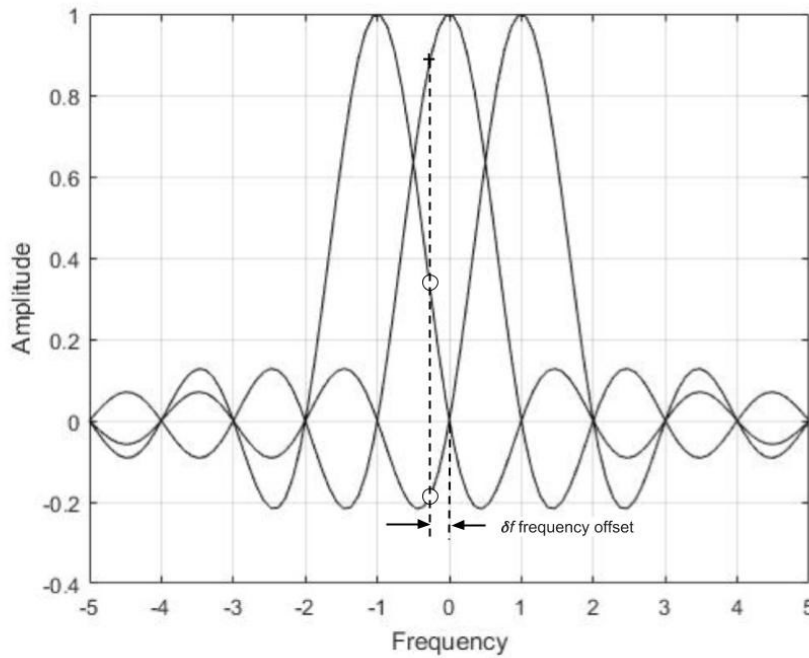


Figure 6. OFDM signal with frequency offset δf causing ICI. The amplitude of the desired sub-carrier is reduced (“+”) and ICI arises from the adjacent sub-carrier (“O”).

A received signal with frequency shift δf and a phase offset θ can be mathematically represented by

$$r'(t) = r(t)e^{j(2\pi\delta ft + \theta)} \quad (1)$$

Where $r(t)$ is a time-variant, multipath fading channel expressed as

$$r(t) = h(\tau, t) * s(t) + n(t) = \int_0^{\tau_{max}} h(\tau, t)s(t - \tau)d\tau + n(t) , \quad (2)$$

$h(\tau, t)$ is the channel impulse response (CIR), $s(t)$ is the complex envelope of the OFDM transmitted signal which is expressed as

$$s(t) = \sum_{k=-\infty}^{\infty} S_k(t - kT), \quad (3)$$

and $n(t)$ is the additive white Gaussian noise (AWGN).

The “*” denoted convolution and the range of integration in the above equation (2) has been limited to $[0, \tau_{max}]$ as CIR is zero elsewhere. τ_{max} is the maximum excess delay of the channel.

The received signal constellation denoted by $y_{i,k}$ thus can be expressed as

$$\begin{aligned} y_{i,k} &= \frac{1}{T_{FFT}} \int_{t=kT}^{kT+T_{FFT}} r(t) e^{j(2\pi\delta f + \theta)} e^{-\frac{j2\pi i(t-kT)}{T_{FFT}}} dt \\ &= e^{j(2\pi\theta)} \frac{1}{T_{FFT}} \int_{t=kT}^{kT+T_{FFT}} \left[\int_0^{\tau_{max}} h(\tau, t) s(t - \tau) d\tau \right. \\ &\quad \left. + n(t) \right] e^{j2\pi\delta f t} e^{-\frac{j2\pi i(t-kT)}{T_{FFT}}} dt \end{aligned} \quad (4)$$

The symbols above are described below:

- T Symbol length, time between two consecutive OFDM symbols,
- T_{FFT} FFT time; effective part of the OFDM symbol;
- k Index of transmitted and received symbol;
- i Index on Subcarrier;
- $y_{i,k}$ Received Signal constellation point, complex symbol modulated on the i th subcarrier of the k th OFDM symbol.

Further, taking into account the transmitted signal constellation $x_{i,k}$ and channel coefficients $h_{i',k}$,

$$y_{i,k} = e^{j(\theta + 2\pi\delta f kT)} \sum_{i'=\frac{N}{2}}^{\frac{N}{2}-1} x_{i',k} h_{i',k} \frac{1}{T_{FFT}} \int_{u=0}^{T_{FFT}} e^{-j2\pi\left(\frac{i-i'}{T_{FFT}} - \delta f\right)u} du + n_{i,k} \quad (5)$$

The integer in the equation (5) is not equal to zero for $i \neq i'$; nor for ideal case $i = i'$, due to frequency error, which implies that the subcarriers have partly lost their orthogonality. The evaluation of above expression yields two terms. The first ($i = i'$) term accounts for equal phase rotation and attenuation of all subcarriers while the second term ($i \neq i'$) describes ICI.

$$\begin{aligned}
y_{i,k} = & e^{j(\theta+2\pi\delta f kT)} x_{i,k} h_{i,k} \frac{1}{T_{FFT}} \int_{u=0}^{T_{FFT}} e^{-j2\pi\delta f u} du \\
& + e^{j(\theta+2\pi\delta f kT)} \sum_{i=\frac{N}{2}}^{\frac{N}{2}-1} x_{i,k} h_{i,k} \frac{1}{T_{FFT}} \int_{u=0}^{T_{FFT}} e^{-j2\pi\left(\frac{i-i'}{T_{FFT}}-\delta f\right)u} du \\
& + n_{i,k}
\end{aligned} \tag{6}$$

The above expressions are valid for a frequency offset of $\delta f < 0.5$ sub-carrier. For larger offsets, the transmitted symbol $x_{i,k}$ gets shifted by one or more positions in the frequency direction, which implies that the i th transmitted data would be seen at $(i + \delta f_i)$ -th subcarrier of receiver, where $\delta f_i = \left\lfloor \frac{\delta f}{F} \right\rfloor$ is the integer part of the frequency error in subcarriers.

Further evaluating the equation (6), we get,

$$y_{i,k} = x_{i,k} h_{i,k} \text{sinc}(\delta f T_{FFT}) \exp\left\{j\left[\theta + 2\pi\delta f\left(kT + \frac{T_{FFT}}{2}\right)\right]\right\} + n'_{i,k} \tag{7}$$

using

$$\begin{aligned}
\frac{1}{T_{FFT}} \int_{t=0}^{T_{FFT}} e^{j2\pi\delta f t} dt &= \frac{1}{j2\pi\delta f T_{FFT}} [e^{j2\pi\delta f T_{FFT}} - 1] \\
&= e^{j2\pi\delta f T_{FFT}} \frac{\sin \pi\delta f T_{FFT}}{\pi\delta f T_{FFT}} = e^{j\pi\delta f T_{FFT}} \text{sinc} \delta f_{FFT}
\end{aligned} \tag{8}$$

The noise term $n'_{i,k}$ in (7) includes the additional due to ICI [27].

2.9 Phase Locked Loop (PLL) CFO Compensation Techniques

As discussed above, synchronization errors such as CFO leads to Inter Carrier Interference (ICI) and to suppress it, CFO compensation is mandatory in the receiver synchronization system. The compensation/estimation of synchronization errors can either be done in time domain or in frequency domain. It is necessary to consider transmissions types, system resources, latency, compensation/estimation accuracy and other factors before using compensation techniques.

In OFDM receivers, the CFO estimation/compensation blocks are phase locked loops. The Time-Domain Derotator and Frequency-Domain Interpolator are two compensation techniques used in OFDM baseband receiver systems which are discussed in detail below. To add in brief, the integer CFO estimation can be done with various algorithms such as time domain correlation, frequency-domain auto-correlation, frequency-domain cross-correlation and frequency-domain PN correlator. The residual CFO can be estimated using Maximum Likelihood (ML) estimator which is popular in MIMO-OFDM systems.

The received continuous time signal is rotated by constant frequency and is in the form,

$$Z_{i,n} = Z(t) e^{j2\pi\Delta f t} \big|_{t=i(N+N_g)T_s+N_gT_s+nT_s}$$

where, Δf is the carrier frequency offset. The CFO can be first normalized with respect to sub carrier spacing ($f_s = 1/(NT_s)$) and then decomposed into integral component (ϵ_I) and fractional component (ϵ_f), that is, $\Delta f = (\epsilon_I + \epsilon_f) f_s$ and $-0.5 < \epsilon_f < 0.5$.

In equation 6, ICI arises due to fractional CFO, ϵ_f . In AWGN channel when the number of subcarrier is large, the SNR degradation due to fractional CFO, D_{SNR} , is given by

$$D_{SNR} \approx \frac{10}{3 \ln 10} (\pi \epsilon_f)^2 \frac{E_s}{N_0} \quad (\text{dB}).$$

To suppress the ICI and thereby reduce SNR degradation, the residual CFO must be sufficiently small. For example, when using 64 QAM constellation, it is better to keep residual CFO below $0.01 f_s$ to ensure that $D_{SNR} < 0.3$ dB for moderate SNR. On the other hand, when QPSK is used, residual CFO can be up to $0.03 f_s$ [15].

A Time-Domain Derotator is commonly used to compensate CFO and to limit residual CFO. The derotator is simply a complex multiplier, which rotates the complex-valued input by a phase shift. The phase derotation is controlled by numerically controlled oscillator (NCO) and is fed to the multiplier as sine or cosine values of the phase. To remove CFO completely, NCO should run at a frequency negative to CFO contained in the received signal but this is not possible as CFO is varying and hidden in the signal with noise and interference. Normally, PLL is adopted in the receiver for estimating and compensating the CFO. Through the feedback loop, the residual error can be maintained at certain limit and the receiver is synchronized with the carrier.

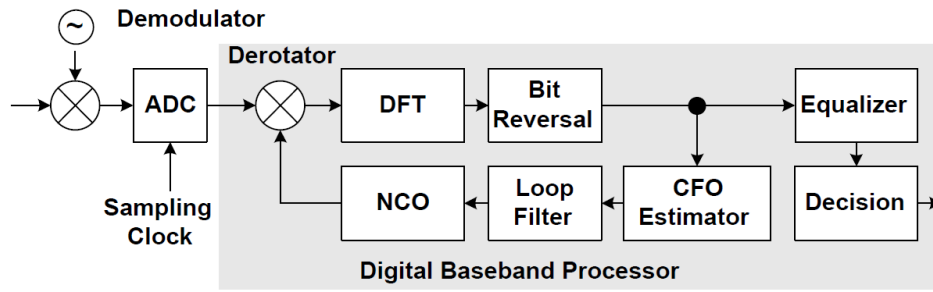


Figure 7. OFDM baseband receiver architecture for CFO compensation using Phase locked loop (PLL) [15].

Figure 7 above shows one baseband receiver for CFO compensation. The CFO estimator in the design is a frequency domain CFO estimator which estimates CFO continuously mixed with noise and interference. The loop filter is used to remove unwanted components and the filtered signal is sent to the NCO, which outputs the digital sinusoidal signal to the complex multiplier.

Another CFO compensation receiver design uses Frequency-Domain Interpolator, which avoids long delays produced by the DFT and bit reversal blocks in the CFO time-domain compensation. The phase rotator used in time-domain is insufficient to be used for frequency-domain receiver signal, since the signal could be corrupted with severe ICI. Therefore, the interpolator is used, which interpolates among the received frequency-domain signals to get signals at the exact frequencies and thereby mitigating ICI. Figure 8 below shows such a receiver design [15].

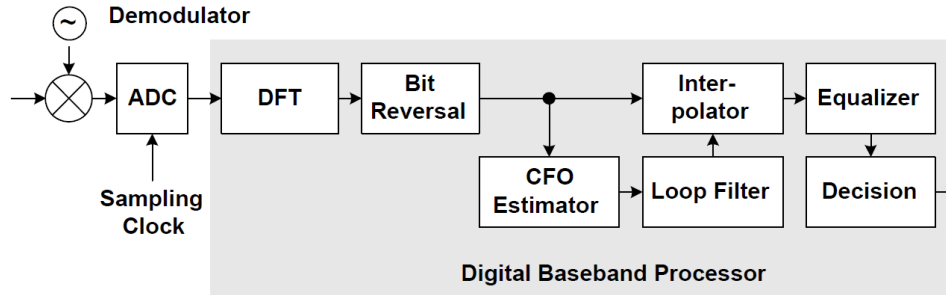


Figure 8. OFDM baseband receiver design using a frequency-domain interpolator to compensate the CFO [15].

2.10 Sampling Clock offset (SCO)

SCO occurs when there is mismatch in oscillator frequency and Doppler Effect. The SCO is similar to CFO as they both originate from the same (oscillator mismatch and Doppler Effect). SCO arises when mismatched frequencies from oscillators are used to drive the sampling clocks of digital to analog convertor (DAC) in transmitter and analog to digital converter (ADC) in receiver. Sometimes, even without sample clock mismatch, the sampled waveform still suffers from error in sampling time because of the movement of transmitter or receiver. The movement of transmitter or receiver causes the waveform to contract or expand in time. This results in Doppler Effect. Figure 9 below shows the sampling error due to frequency mismatch and Doppler Effect.

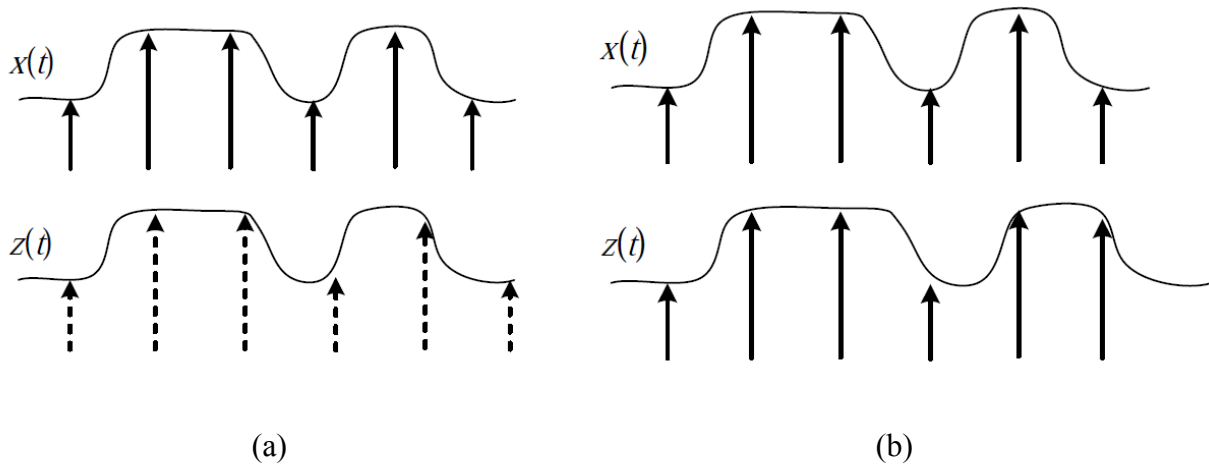


Figure 9. (a) Sampling error due to sampling of transmitted signal $x(t)$ and received signal $z(t)$ at different clock rates. (b) Received signal $z(t)$ is expanded due to Doppler effect, resulting in sampling error even without clock rate mismatch.

Figure 9 (a) depicts the sampling error due to different clock rates of transmitted and received signal, which causes the received signal to be sampled at time instances that are progressively skewing. Figure 9 (b) shows sampling error due to Doppler Effect as motion between transmitter and receiver causes the signal waveform to expand or contract in time.

Mathematically, if the received is sampled at interval of $(1+\delta) T_s$ instead of ideal T_s , then the n th received sample of the i th symbol can be written as

$$Z_{i,n} = Z(t)|_{t=i(N+N_g)(1+\delta)T_s+N_g(1+\delta)T_s+n(1+\delta)T_s}, \quad \text{for } n = -N_g, \dots, N-1. \quad (1)$$

where,

T_s = ideal sampling time,

N = window interval,

N_g = window with guard interval,
 δ = sampling clock offset.

Assuming that there is no ISI contamination in DFT window, the k th frequency-domain received signal of the i th symbol is given by,

$$\begin{aligned}
Z_{i,k} = & X_{i,k} H_k \frac{\sin(\pi\delta k)}{N \sin\left(\frac{\pi\delta k}{N}\right)} e^{j2\pi \frac{i(N+N_g)+N_g}{N} \delta k} e^{j\pi \frac{N-1}{N} \delta k} \\
& + \sum_{l=-\frac{N}{2}-1}^{\frac{N}{2}-1, l \neq k} X_{i,l} H_l \frac{\sin(\pi((1+\delta)l-k))}{N \sin\left(\frac{\pi((1+\delta)l-k)}{N}\right)} e^{j2\pi \frac{i(N+N_g)+N_g}{N} \delta l} e^{j\pi \frac{N-1}{N} [(1+\delta)l-k]} \\
& + n_{i,k}
\end{aligned} \tag{2}$$

where,

$X_{i,k}$ = k th complex-valued frequency-domain signal of the i th symbol,
 H_k = channel frequency response,
 $n_{i,k}$ = channel noise component in the k th subcarrier of the i th symbol.

The first term in the received signals (equation 2) clearly shows that the sampling offset, δ , causes phase shift and magnitude attenuation in the transmitted signal. The above equation also depicts that phase shift has constant increment proportional to k and δ as symbol index i increases. Moreover, ICI is also introduced in the above equation (2), which is represented by the second term [15].

2.11 Software Defined Radio (SDR)

Software-defined radio (SDR) is a radio communication system that replaces partially or fully traditionally implemented hardwares (e.g. mixers, amplifiers, modulator/demodulator, detectors) by means of software on a personal computer or embedded system. SDR can model and control complicated analog RF tasks, such as modulation and demodulation, simply by using software and programming environments.

USRP N200 series is a high performance USRP device designed and produced by Ettus research that provides high bandwidth and high dynamic range. It operates from DC to 6 GHz. Data streaming and programming of device can be done through gigabit Ethernet port. It provides sampling rate up to 50 MS/s to and from host applications.

USRP hardware

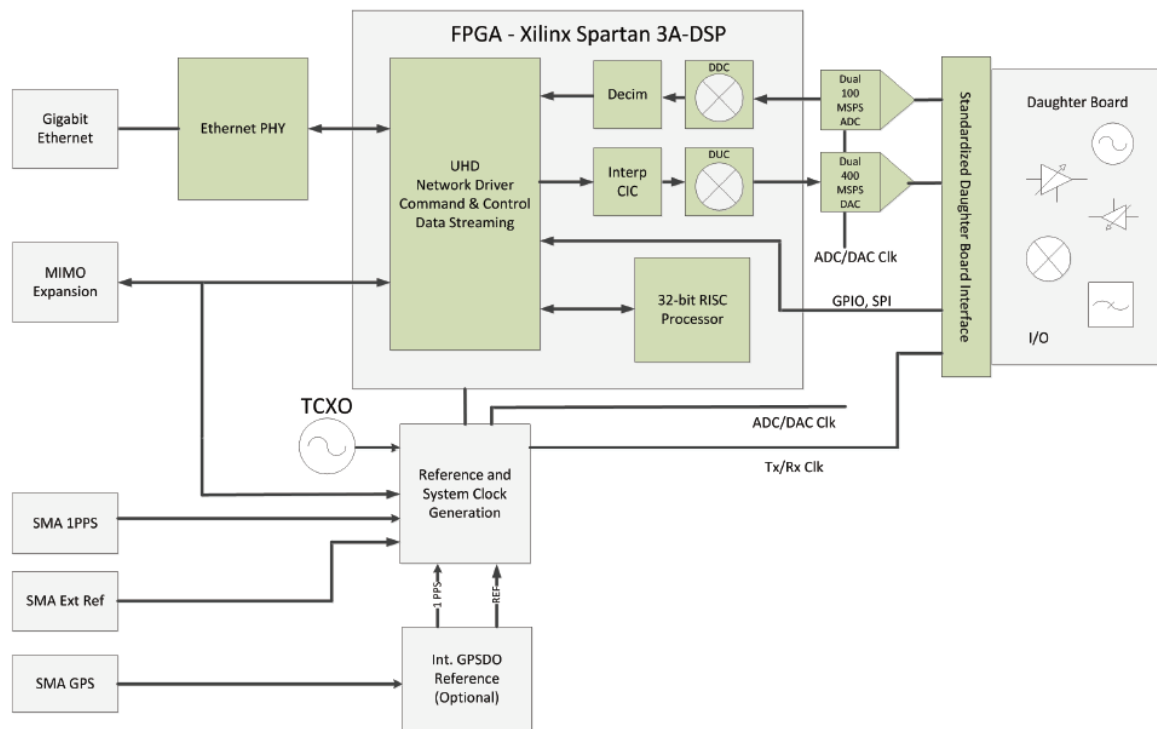


Figure 10. Internal Architecture of USRP Device [16].

The main hardware inside a USRP unit mainly consists of a Field-Programmable Gate Array (FPGA) with Digital Signal Processing (DSP) functionality. Furthermore, the hardware includes multiple high-speed ADCs for sampling a received signal and high-speed DACs for generating a signal for transmission. The FPGA configures a local oscillator to the desired carrier frequency and processes the samples to and from the DACs and ADCs from the incoming or outgoing data on the Ethernet link. Some of the USRP modules include a high-precision clock as the clock reference. The USRP module has two options for clock reference: internal GPS disciplined oscillator (GPSDO) or external reference clock signal. In general, the USRP main hardware supports any carrier frequency between DC and 6 GHz usually, only limited by the actual RF frontend.

The USRP N200-KIT module used within this document has following specifications:

- ADCs: 100 MS/s 14-bit
- DACs: 400 MS/s 16-bit
- Mixer: programmable decimation- and interpolation factors
- Max. BW: 50 MHz
- PC connection: Gigabit Ethernet connectivity
- RF range: DC – 5.9 GHz, defined through RF daughterboard

The architecture of the software radio in Fig.10, common reference and system clock drives both daughter board (Tx/Rx clk) and ADC/DAC (ADC/DAC clk) hardware section of USRP unit. The ADC/DAC unit is responsible for sampling incoming and outgoing signals and daughter board transmits and receives radio signal at desired carrier frequencies. Thus, same reference clock signal affects carrier frequency as well as sampling frequency in USRP unit. Therefore, when feeding external clock with errors to the USRP units, the CFO and sampling errors occurs in the signal generated. The CFO and sampling errors correlate each other since they have common reference clock signal and thus compensation of these errors is difficult.

USRP Clock Precision

USRP needs a reference clock source that distributes the clock signals to the functional components such as ADC, DAC, FPGA, motherboard and daughterboard. The standard reference clock source frequency is 10 MHz. It is important that the reference clock source is precise and accurate so that the devices and components works with exact same frequency and time.

The USRP used in this thesis work is N2x0 which is manufactured by Ettus Research. Ettus research specializes in Software Defined Radios (SDR) systems. Ettus produces broad range of USRPs some of which are USRP X series (USRP X300, USRP X310), USRP Networked series (N200, N210) and USRP E series (310, 312, 313). Each of the USRPs have key features and specifications and they can be selected that fulfills the research requirements. This thesis work uses USRP Networked series (N200, N210) because of its features such as RF range up to 6

GHz, bandwidth of 40 MHz, gigabit Ethernet interface, MIMO capability and external clock reference. The USRP platform addresses a wide range of RF applications from DC to 6 GHz.

The key features of N2x0 in terms of reference clock source are as follows:

- it has ability to lock to external 5 or 10 MHz clock reference,
- it has temperature compensated crystal oscillator (TCXO) frequency reference which provides accuracy of 2.5 ppm.
- It also has an optional internal GPS locked reference oscillator (GPSDO) which provides accuracy of 0.01 ppm.

The reference and system clock generation block of USRP architecture takes the reference clock source from one of the source (external, TCXO and GPSDO) and distributes the clock signals to FPGA block, ADC/DAC block and daughter board. The clock signal is essential to these blocks as processing and sampling is done in every pulse or edge of the clock signal. The signal processing, sampling and trans receiving of signals are all driven by reference clock signals. Therefore, precise clock signal source is required for best performance of the USRP.

The external reference clock signal can be connected to USRP through SMA Ext Ref. Pulse Per Second (PPS) signal can also be provided to USRP through SMA 1 PPS. The reference clock requires power level of 0 to 15 dB for N2x0 and if PPS signal is used then amplitude required is 3.3 to 5Vpp. In this thesis work, external reference clock signal is used which is generated from signal generators. The standard 10 MHz clock signal is generated from signal generators and it is fed as external clock signal to USRP. The precision of signal produced by signal generators is 0.01 ppm ($1 * 10^{-8}$) since they use oven controlled crystal oscillator (OCXO) as internal clock oscillator [30].

Similarly, USRP internal oscillator TCXO can also be used as a clock signal reference which provides precision of up to 2.5 ppm [28]. The standard 10 MHz clock signal is generated by TCXO and distributed throughout the USRP blocks. The fact that internal oscillator is not used in this thesis is because the clock signal frequencies cannot be varied for two USRPs to produce clock errors between them.

USRPs also have an option to use GPSDO to provide clock signals to USRP blocks. This option is available in newer and advanced USRPs and N2x0 also has this option. GPSDO provides accuracy of up to 0.01 ppm [29]. The GPSDO has a combination of GPS receiver and high stable oscillator such as quartz or rubidium oscillator. The output is controlled to agree with signal broadcast by GPS or GNSS satellites.

A GPS antenna is required to be attached to USRP to receive GPS signals if GPSDO is used as reference clock. By default, if GPSDO is detected at startup, the USRP is configured to use it as a frequency and time reference. The internal oscillator of USRP is phased locked to the 10 MHz GPSDO reference. GPSDO acts as a source of timing and it is accurate because the satellite signals must be accurate in order to provide position accuracy for GPS navigation. These signals are accurate to nanoseconds and provide good reference for timing applications.

The specifications of N2x0 and internal GPSDO and Rhode & Schwartz signal generators can be found in appendix B.

3. Measurement System Description

3.1 Measurement Setup

The main purpose of this thesis work is to study the impact of clock error in the radio link performance of NB-IoT system. The methodology used for this work is to insert clock error in the system, measure and collect uplink data and signal information shared between UE and eNodeB. The analysis of signal information would show the effect of clock error in the system and behavior of the radio link between UE and eNodeB when clock error is introduced.

The system used here is a NB-IoT, which has been implemented in the LTE stack on flexible software radios based C-RAN testbed [8]. The radio signal is transmitted over the wire between UE and eNodeB instead of over the air to protect the link from interference and unintended attenuation. The frequency band used in the system for uplink is 635 MHz and for downlink 640 MHz. The UE and eNodeB connects with each other through information exchange and physical channels interaction. The physical channels in the NB-IoT system are briefly described in the chapter 2.2.

UE initiates random-access procedure whenever it wants to transmit data in the network. The random-access procedure consists of four steps: (1) UE transmits a random-access preamble; (2) the network transmits a random-access response that contains timing advance command and scheduling of uplink resources for the UE; (3) the UE transmits its identity to the network using the scheduled resources and (4) the network transmits a contention-resolution message to resolve any contention due to multiple UEs transmitting the same random access preamble in the first step. The random access achieves uplink synchronization which is important for uplink orthogonality in NB-IoT [5].

In the measurement, the eNodeB schedules one UE in each uplink transmission opportunity. The maximum number of repetition is $R = 128$. In each window, the BS allocates 2 resource units for NB-PUSCH. The repetition pattern of NB-PUSCH follows a cyclic sub frame level repetition where in each cycle, each of the scheduled sub frames is repeated $Z = \min(4, R) = 4$ times. To save power, the eNodeB attempts to decode NB-PUSCH data after every fourth repetitions. In case of early decoding, the remaining uplink repetitions are discarded. The number of repetitions that are required to successfully decode the uplink data depends on the received SNR and the channel coherence time [8].

USRP A (eNodeB) and USRP B (UE) are fed with standard 10 MHz external clock signals coming out from signal generators. The connection is presented in the Fig. 11. The Analog to Digital converter (ADC) or Digital to Analog Converter (DAC) of USRP A and USRP B are when fed with different frequency clock signals, the clock offset is introduced in the system.

The carrier offset and sampling offset are introduced as well in the system. The offsets are described briefly in the chapter 2.

The standard 10 MHz external clock signals are generated using Rhode & Schwartz signal generators in a master- slave configuration.

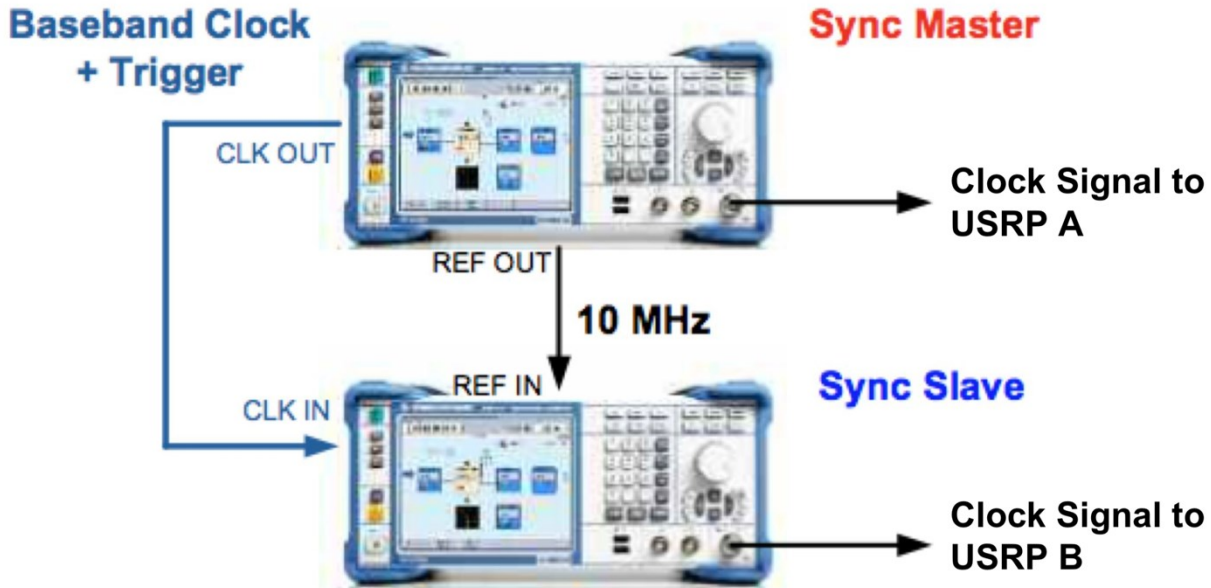


Figure 11. Time synchronous signal master-slave setup [21]

The connection of the set-up is carried out from equipment's manual [21]. The cabling of signal generators is important to produce synchronous signals. The CLK OUT of master is connected to CLK IN of slave and the REF OUT of master is connected to REF IN of slave. The clock is set as internal in master and external in slave. The frequency of the distributed clock signal is 50 MHz. The reference oscillator source is set as internal in master and external in slave. The reference oscillator frequency is 10 MHz and is distributed among slave by the master. The master-slave setup produces 10 MHz synchronized signals. It is possible to create offset in the synchronized signal simply by changing frequency of the slave. Digital oscilloscope and spectrum analyzer were used to check that the signals are synchronous and 10 MHz in frequency.

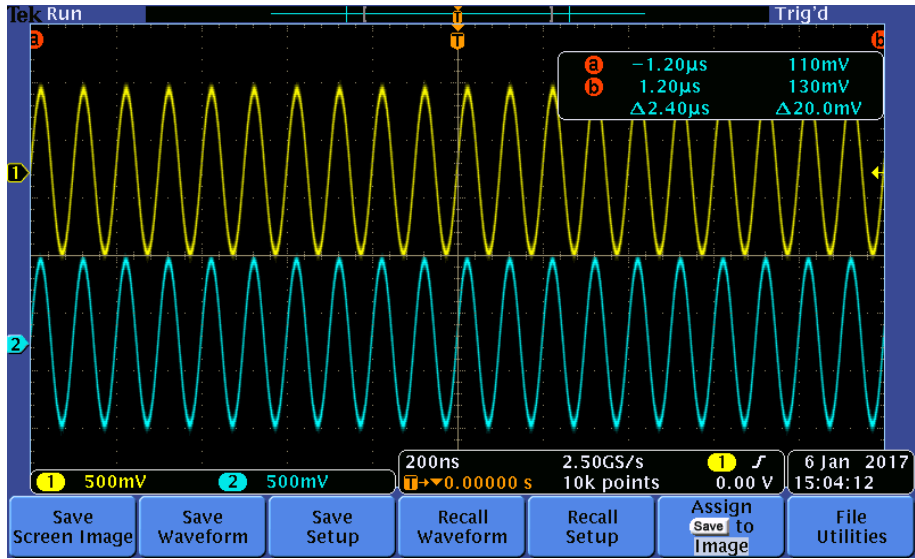


Figure 12. Digital oscilloscope Signals of master and slave at 10 MHz (scale: 200ns)

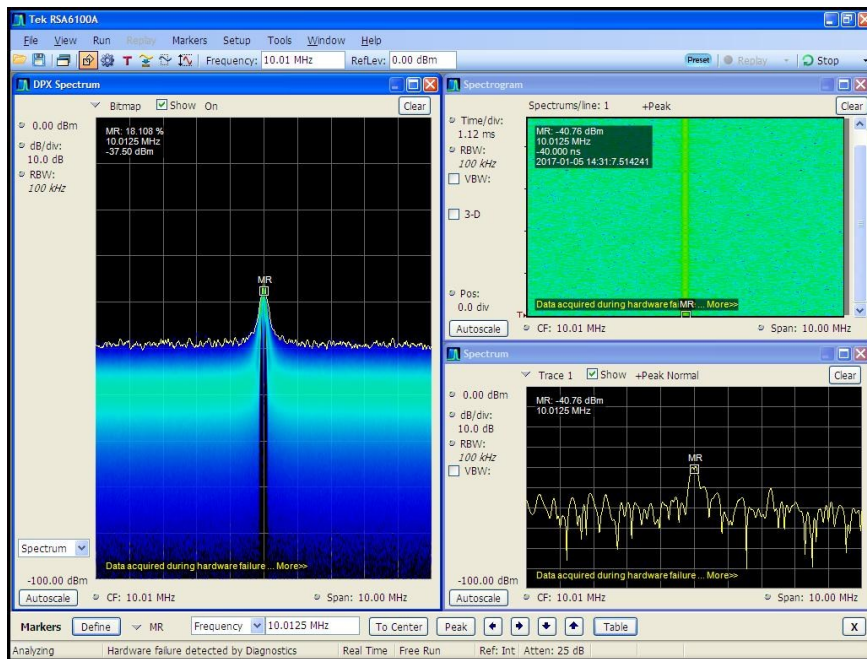


Figure 13. Spectrum analyzer showing master signal center frequency at 10 MHz

During the measurement, the master signal is fed as clock signal to USRP A and slave signal is fed as clock signal to USRP B. The clock signal drives the local clock present in the USRP's.

The clock frequency of slave is gradually increased by 1 Hz by changing the frequency in the slave signal generator. This created offset in the clock signal fed to USRPs which is known as clock offset. The clock offset of up to 12 Hz is generated between eNodeB and UE. At this range, the UE and eNodeB shows good synchronization with each other. Most of the data packets are received by eNodeB that is sent by UE (i.e. 90% of the data packets). When the clock offset exceeds 12Hz, the UE and eNodeB has difficulty to synchronize and there is connection breach sometimes. The packet drop is high above 60% to 70%. After 15Hz, UE and eNodeB do not synchronize at all and all packets are dropped by the eNodeB.

Every time the clock offset is introduced in the system, the carrier frequency offset (CFO) is introduced as well. Every 1 Hz of clock offset, introduces 100's of Hz of CFO in the system. At 12 Hz, CFO is already 805 Hz for carrier frequency band of 640 MHz [chapter 4.2], which is high. Therefore, after certain clock offset, the UE and eNodeB are not able to synchronize at all. The change in CFO to the change in clock offset is presented in the chapter 4.2.

The system is implemented with 3 different MCS index [0, 3 and 6]. For each parameter [0, 3, 6], 12 samples were taken at different clock offsets (1 Hz to 12 Hz). The UE transmits data packets in Uplink with given MCS indexes [0, 3, 6] to eNodeB. The aim here is to observe the performance of the radio link at various modulation techniques and coding rates. MCS index has been described in brief in chapter 2.5.

For each MCS index, the measurements are taken at various signal strengths typically ranging from -110 dB to -86 dB. The received signal strength of -110 dB is weak but acceptable for data transmission and reception. The received signal of -86 dB is a strong signal. This range of signal strength provides good understanding of radio link performance which is under study. With this range of received signal level, the SINR typically ranges from -12 dB to 12 dB. The number of repetitions that are required to successfully decode the uplink data by eNodeB is stored for each signal level.

After collecting measurement data's, the work is to find out the clock error impact on the radio link performance of NB-IoT test bed. The data collected from the measurement are processed in the Matlab for the analysis. The analysis includes the change in the received power, number of retransmissions, BLER and SINR to the change in signal strength and clock error for various MCS values. The graphs are plotted and thorough analysis is done to understand the system behavior and performance for the effect of clock offset introduced in the system.

Measurements require few important devices and proper connection within themselves and with the server. The devices used for the measurement are as follows as seen in the Fig. 14. A brief introduction of the devices is provided in appendix C.

1. Two USRP N200 (one is used as eNodeB and other as User Equipment (UE))
2. Step Attenuator
3. Two signal generators
4. Real time spectrum analyzer
5. Digital Oscilloscope and
6. A server (Desktop)

The overall configuration of the setup is show below via diagram.

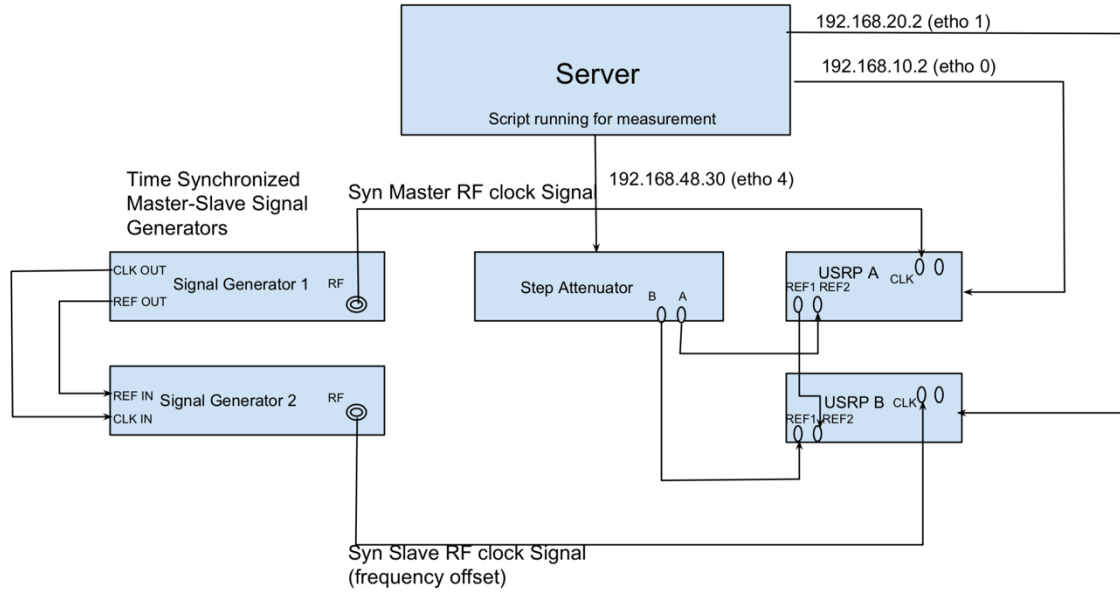


Figure 14. Overall setup for the measurement

The server is connected to two USRP's and step attenuator via Ethernet port with connection names etho 0, etho 1 and etho 4. The ip addresses of USRPs and step attenuator can be found in appendix D.

There is a radio signal connection between USRP A, USRP B and step attenuator. The Tx of USRP A is connected to Rx of USRP B. The Rx of USRP A and the Tx of USRP B is connected to node A and B of step attenuator. Sometimes, there can be a loose connection of wires to and from transmitter and receiver of USRP's. The wires are impedance matched and loose wire may have effect in receiving and transmitting power of the signal which may affect the analysis and result of the measurement. Therefore, the wires are tightened properly and leakage of power is prevented.

3.2 Measurement Configuration

The NB-IoT test bed used in this thesis work is implemented on a flexible SDR based C-RAN. This C-RAN technology runs in the host server. The executable files initiate SDR to run as eNodeB and UE within the network. The eNodeB runs with three different MCS indexes [0, 3, 6]. UE communicates consecutively with eNodeB having MCS index [0, 3 and 6]. The script has been written to control the overall setup and measurement. The step attenuator is remotely controlled as well for various signal strength ranging from -110 dB to -86 dB. Data are stored in several text files which are then processed and analyzed using Matlab script. The Matlab script processes the sample data, removes undesired information's, calculates BLER and SINR and finally produces plot to see the impact of clock error in the radio link performance.

The measurement was taken for 12 times with clock error ranging from 1 Hz to 12 Hz. Each time, the frequency of slave signal generator was increased by 1 Hz and the script was run to collect data's. Altogether, 12 sample data files were collected.

3.3 Measurement Data Processing

The information is stored in a text file which includes timestamp of the signal, flag showing successful decoding of the received signal, number of retransmissions or decoding attempts (R), RSSI (Received Signal Strength Indicator) value and SINR of the signal. All these values are extracted, processed and stored in Matlab for analysis.

UE stores the necessary information about transmission and timestamp of the transmitted packet. eNodeB stores the timestamp, flag, rep (R), RSSI, SINR and error for warning. The timestamp of data packet sent by UE must equal to timestamp of data packet received by eNodeB to be a valid data packet. The timestamp of sample data from both UE and eNodeB is compared. If timestamp is matched, the data is considered as valid and if it does not match, the data is considered as invalid and not taken into consideration for analysis.

The UE transmits data packets several times to eNodeB. The number of retransmissions or decoding attempts (R) ranges from 1 to 128. The retransmission of packets is done in multiple of 4. eNodeB decodes the received packets and number of decoding attempts are stored for each data packet.

The RSSI value shows the relative signal power strength of the received signal which ranges from -100 to 0 in arbitrary unit. The eNodeB calculates RSSI value from preamble stage of receiving a data frame and is stored in text file. RSSI is an indication of received power level after antenna and possible cable loss. Thus, higher the RSSI number, the stronger the signal. With the help of RSSI value, the noise floor (N) and received power (Pr) is calculated and stored using Matlab script. The SINR (γ) value shows the signal to interference plus noise ratio of the signal. SINR (γ) is calculated using received power and noise floor (i.e. $\gamma = Pr - N$).

The UE transmits around 3750 packets for each received power level after the connection has been established between UE and eNodeB. For each MCS index and 25 different received power level, total of 93,750 packets are transmitted by UE to eNodeB. Nearly 10% packets are dropped during analysis when clock error is 1 Hz because of timestamp mismatch and non-decoded packets at eNodeB.

3.4 Issues during the measurement

One of the issue during the measurement was to generate synchronized clock signal of 10 MHz that is fed as external clock signal to USRPs. The external clock signal serves to keep the local oscillator phased lock to 10 MHz signal. For this purpose, signals generators were used and the setup was done as per guideline provided by the manufacturer (Rohde and Schwarz SMBV100a signal generators were used in the measurement). The setup is explained in chapter 3.1. The baseband signal modulation for time synchronous signals as per guidelines from manufacturer includes the modulation of radio frequency signal. The modulated signal contains multiple peak frequencies. Such a modulated signal when used as clock signal to drive the local clock of USRP would create conflict on which one of the multiple peak frequencies to use to drive the clock. So, simple synchronized signals are used as external clock frequency signal to feed URSP's local clock.

The second issue in the measurement was to find out the range of clock error that is fed to the USRPs. The range was specified from 1 Hz to 12 Hz after number of tests. The external clock signal fed to USRPs was varied each time by 1 Hz, and the synchronization status of UE and eNodeB was checked. UE and eNodeB remained synchronized up to 12 Hz of clock error. Clock error greater than 12 Hz resulted in interrupted and discontinuous synchronization between UE and eNodeB and above 15 Hz, the UE and eNodeB did not synchronize at all.

4. Measurement Analysis

4.1 Change in Clock error to the change in Carrier Frequency Offset (CFO).

The external clock signal fed to USRP devices drives the local clock to be phase locked with its frequency. If there is frequency mismatch between clock signals fed to USRPs, then the received signal is shifted in frequency than the actual transmitted signal which is known as CFO. Even small frequency error leads to CFO of several Hz as presented in Table 5. The detailed explanation about CFO is present in chapter 2.7. The table below summarizes the change in CFO corresponding to clock error. The system did not synchronize at all when the clock error/offset was higher than 14 Hz.

Table 5. Clock errors and corresponding CFO for 640 MHz, 963 MHz and 1800 MHz.

Clock error in Hz (Clock frequency- 10MHz)	CFO for 640 MHz in Hz / ppm	CFO for 963 MHz in Hz / ppm	CFO for 1800 MHz in Hz / ppm
0	33 / 0.051	65 / 0.067	130 / 0.072
1	95 / 0.148	165 / 0.171	310 / 0.172
2	159 / 0.248	255 / 0.264	490 / 0.272
3	223 / 0.348	355 / 0.368	670 / 0.372
4	289 / 0.451	455 / 0.472	852 / 0.473
5	353 / 0.551	546 / 0.566	1032 / 0.573
6	415 / 0.648	646 / 0.670	1212 / 0.673
7	480 / 0.750	736 / 0.764	1373 / 0.762
8	534 / 0.834	836 / 0.868	1573 / 0.873
9	613 / 0.957	936 / 0.971	1754 / 0.974
10	677 / 1.057	1027 / 1.066	1914 / 1.063
11	741 / 1.157	1127 / 1.170	2094 / 1.163
12	805 / 1.257	1227 / 1.274	2295 / 1.275

The measurements in the above Table 5 are taken for frequencies of 640 MHz, 963 MHz and 1800 MHz. The above frequencies are interesting because the testbed used for measurements use 640 MHz as downlink frequency and other frequencies (963 MHz and 1800 MHz) are used for cellular networks (GSM, UMTS and LTE bands). Since, NB-IoT is going to be deployed in GSM and LTE networks, it is interesting to see how much CFO is produced by clock errors in those frequency bands (963 and 1800 MHz).

It is seen in Table 5 that there is small CFO (33 Hz for 640 MHz) with no clock error. As error is increased, the CFO increased significantly. The CFO increases from 33 Hz to 805 Hz as offset rise from 1 Hz to 12 Hz for 640 MHz. Increase in clock error of 1 Hz nearly increased CFO by 65Hz for 640 MHz. Similarly, for 963 and 1800 MHz, the increase in CFO was nearly 100 Hz and 200 Hz. It can be observed from above table that higher the carrier frequency, higher is the CFO with small clock error.

The effect of higher clock frequency error resulted in higher CFO that generated problems such as difficulty in synchronization between eNodeB and UE, higher packet loss and higher retransmissions of data between UE and eNodeB.

Clock error was introduced in the measurement ranging from 1 Hz to 12 Hz. The clock frequency of 10 MHz was fed to USRPs. It is often preferred to denote clock errors in parts per million (ppm) or parts per billion (ppb) rather than in Hz. Error in Hz can be converted to ppm
$$\frac{(\text{error frequency}) * 10^6}{(\text{clock frequency})}$$
.

For example, error frequency = 1 Hz, clock frequency = $10 * 10^6$ Hz, so 1 Hz error is equal to $\left[\frac{(1 * 10^6)}{(10 * 10^6)} \right] = 0.1 \text{ ppm}$. Similarly, 10 Hz error is equal to 1 ppm and 12 Hz error is equal to 1.2 ppm.

In the above Table 5, CFO errors are denoted in Hz and ppm. For clock error of 1 Hz at 640 MHz, CFO is 95 Hz which is equal to ~ 0.15 ppm. Similarly, for 12 Hz clock error, CFO is 805 Hz which is equal to 1.25 ppm.

4.2 Analysis of Measurement Data

From the measurement data, important and interesting parameters are computed such as SINR, R, Pr and BLER. The brief introduction of parameters is presented in chapter 3.3.

As discussed in chapter 4.1, the clock error increases CFO of the system which generates difficulty in synchronization between eNodeB and UE because received signal is shifted in frequency (due to offset) than the original transmitted signal. Also, the clock error produces the sampling offset which is discussed briefly in chapter 2.10. The offsets and synchronization issue leads to data packets loss. Therefore, this thesis work selects the parameters mentioned above to observe the impact of clock error in the radio link of the NB-IoT system. Moreover, NB-IoT

achieves coverage extension through retransmissions of packets which generates more interest for the parameter R for analysis.

The analysis shows that for nearly 89% of the packets are correctly decoded by the eNodeB when the clock error is 1 Hz whereas only 49% of the packets are decoded when the clock error rises to 12 Hz for MCS index 0. Another interesting data observed is that, in average 99.4 retransmission of packets is required out of 128 at SINR of -11.7 dB for clock error 1 Hz whereas 128 or more retransmissions of packets is required when the clock error is 12 Hz. The minimum retransmissions of packets are 4 which generally occurs when the received signal is strong and SINR of the signal is high. For example, as seen in the Fig.15 for clock error of 1 Hz, the average value of R is 4 when the SINR is around 5dB. The above values are true for MCS index 0. It is observed in Fig.16 that when MCS index is 3 or 6, the minimum retransmissions (i.e R=4) is never reached as the higher MCS index has weak protection against packet loss. Below Table 6 shows some statistics from processed data which are briefly discusses in the paragraph.

Table 6. Statistics showing average retransmissions (R), number of packets decoded and SINR for different clock error and MCS index.

Clock error	MCS Index	Average Retransmissions (R)	number of packets decoded correctly	Min. SINR and Max. SINR
1 Hz	0	99.34 4	200 3748	-11.7 12.3
	3	128 or failed* 4	3747 3748	-11.69 12.31
	6	128 or failed* 4	3747 3748	-11.69 12.3
12 Hz	0	128 or failed* 4	2086 2089	-11.9 12.1
	3	128 or failed* 6.45	2064 1969	-11.6 12.05
	6	128 or failed* 12.23	1996 1663	-11.87 12.12

*failed – implies none of the packets were decoded successfully.

The boxplot below shows distribution of R over SINR values for MCS indexes. The first quartile and third quartile are the 25th and 75th percentile of the sample data respectively with confidence interval of 50%.

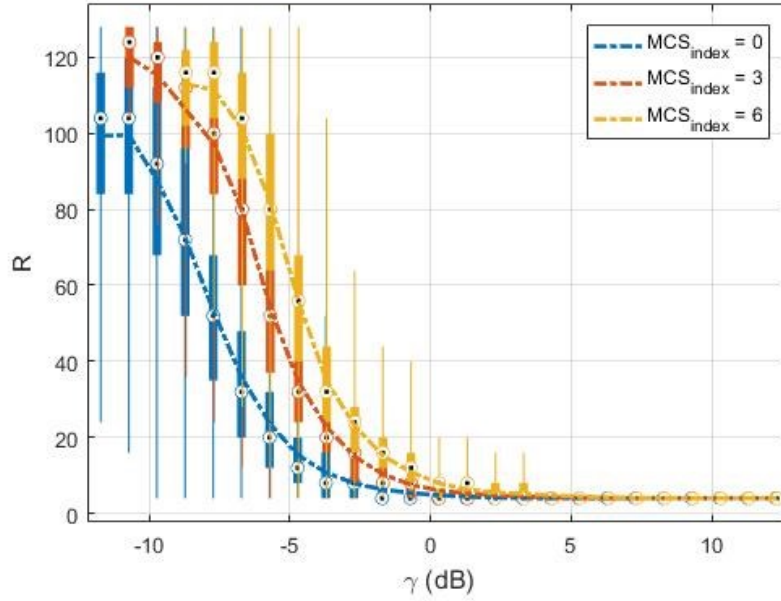


Figure 15. Box plot showing distribution of R over SINR(γ) for clock error of 1 Hz.

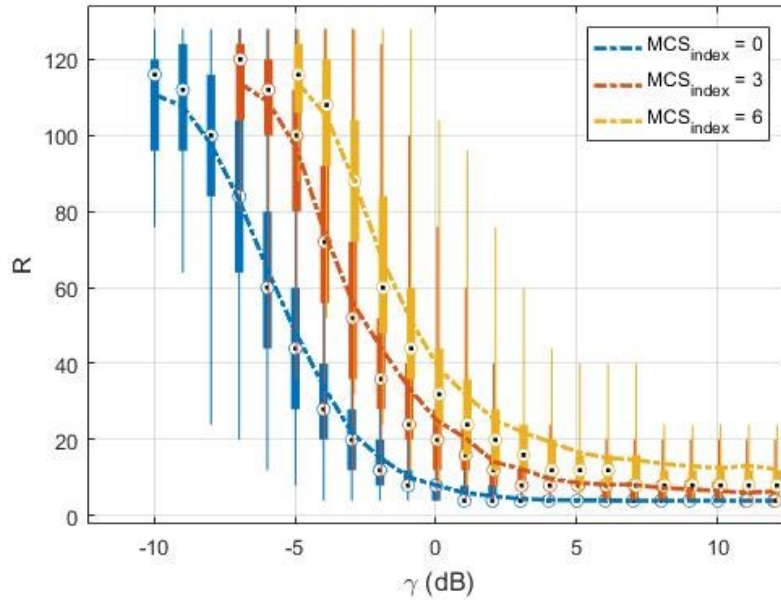


Figure 16. Box plot showing distribution of R over SINR(γ) for clock error of 12 Hz.

The plot below (Fig.17 (a) and (b)) shows similar behavior as discussed above but with logarithmic scale for R. The curves show that retransmissions of packets are low for MCS index 0 than MCS index 3 and 6 for same SINR value. For example, when SINR is -5 dB, retransmissions $R \approx 20$ for MCS index 0 while $R \approx 40$ and $R \approx 60$ for MCS index 3 and 6. The above-mentioned values are true for clock error of 1 Hz. Also, it is observed that the minimum retransmissions R for MCS=3 and MCS=6 increases abruptly as the clock error increases. Figure 17 (b) shows that retransmissions $R \approx 50$ for MCS index 0 while $R \approx 100$ and $R \approx 115$ for MCS index 3 and 6 for clock error of 12 Hz. The high retransmissions is due to the fact that increased clock error produces CFO and synchronization issue which leads to higher packet loss.

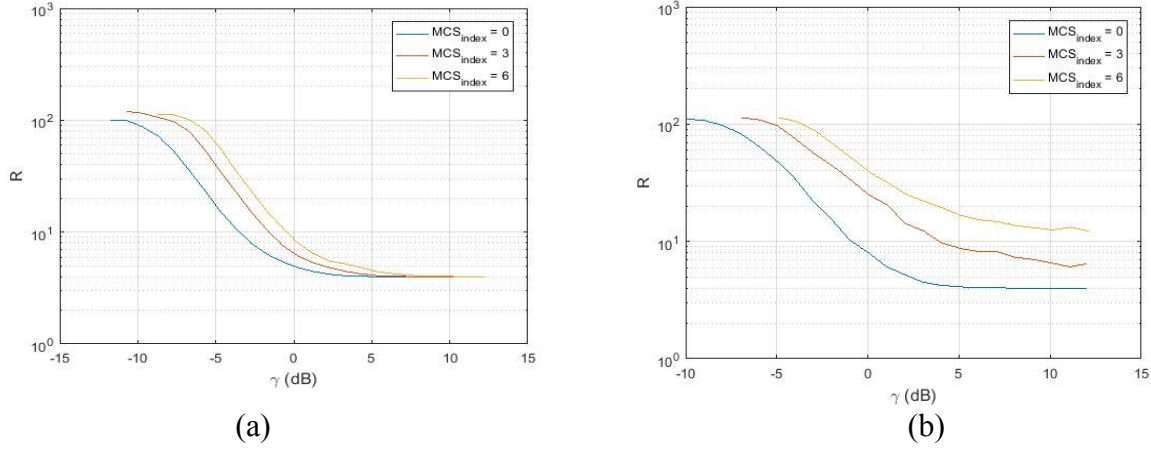


Figure 17. (a) Plot showing SINR(γ) vs average retransmissions (R) for clock error of 1 Hz.
(b) Plot showing SINR(γ) vs average retransmissions (R) for clock error of 12 Hz.

BLER is another important parameter to analyze to observe packet drops due to clock error. Table 7 below shows the BLER statistics at clock error of 1 Hz and 12 Hz. The BLER increases significantly as clock error rises. There is around 18% increase in error packets as clock error rises from 1 Hz to 12 Hz for MCS index 6 at strongest signal of SINR 12 dB. When clock error is 12Hz and MCS index is 6, BLER is 1 for SINR -11.7 dB to -5.7 dB and even during the strongest signal (i.e. SINR 12.3 dB) BLER is above 0 (0.1792). If that is to be compared with clock error of 1 Hz, even for MCS 6, BLER is 0 for SINR -4.7 dB and above. This implies that as clock error rises and MCS index is high, the data packets are more vulnerable to errors even though the signal strength is strong. The error is mainly because of synchronization problem between UE and eNodeB at high clock error.

Table 7. Statistics showing BLER and SINR for different clock error and MCS index.

Clock error	MCS Index	BLER	Min. SINR and Max. SINR at which BLER > 0
1 Hz	0	0.9466 0.0264	-11.7 -5.5
	3	1 0.0035	-11.69 -5.5
	6	1 0.0029	-11.69 -6.5
12 Hz	0	1 0.0062	-11.6 -7.5
	3	1 0.0015	-11.6 2.1
	6	1 0.1792	-11.87 12.3

The graphs below depict the relation of BLER with SINR. The plot in Fig.18 shows that for clock error of 1 Hz and MCS index 0, BLER drops by around 50% every time SINR is increased by 1 dB up to certain SINR value (-5.7 dB). After that BLER drops to 0 as SINR increases. Figure 19 depicts clock error at 12 Hz where BLER is undesirably high mainly for MCS index 3 and 6. The clock error rise affects the radio link and its performance leading to packet drops. The packets are more vulnerable to error in case of MCS index 3 and 6.

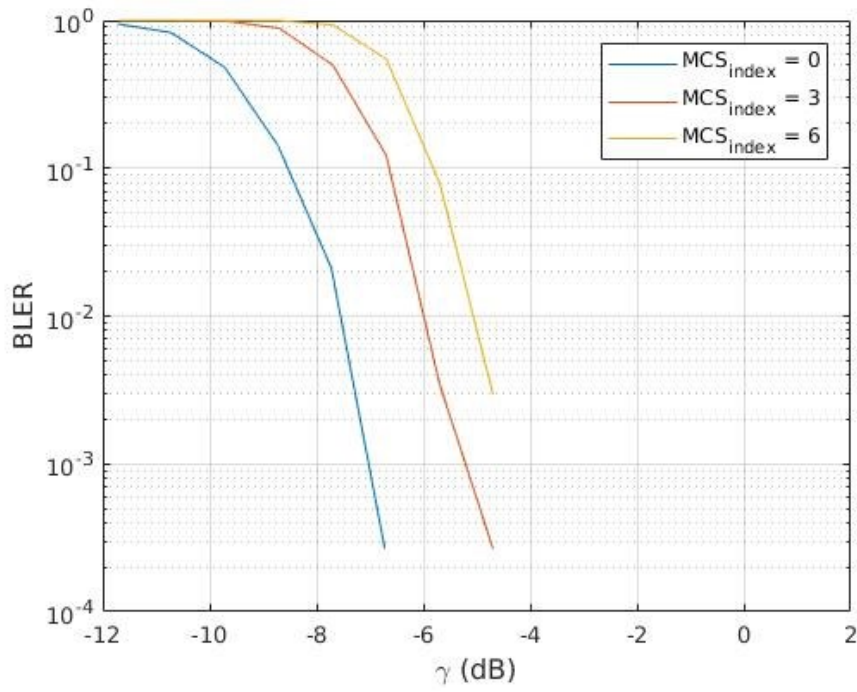


Figure 18. Plot showing SINR(γ) vs BLER for clock error of 1 Hz.

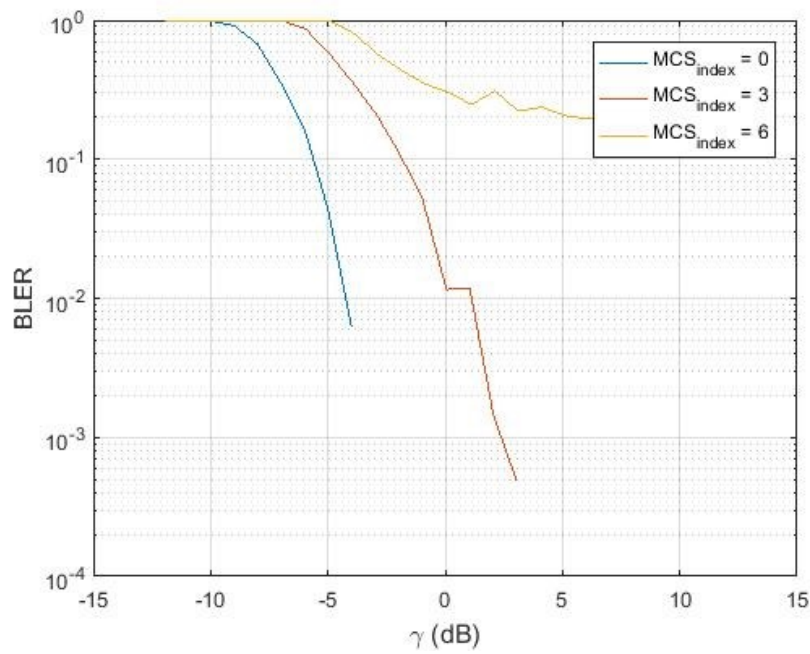


Figure 19. Plot showing SINR(γ) vs BLER for clock error of 12 Hz.

In Fig. 20 (a) and (b) below, BLER ranges from 0 to 1, distinctly showing BLER drop at SINR values for MCS index [0, 3 and 6].

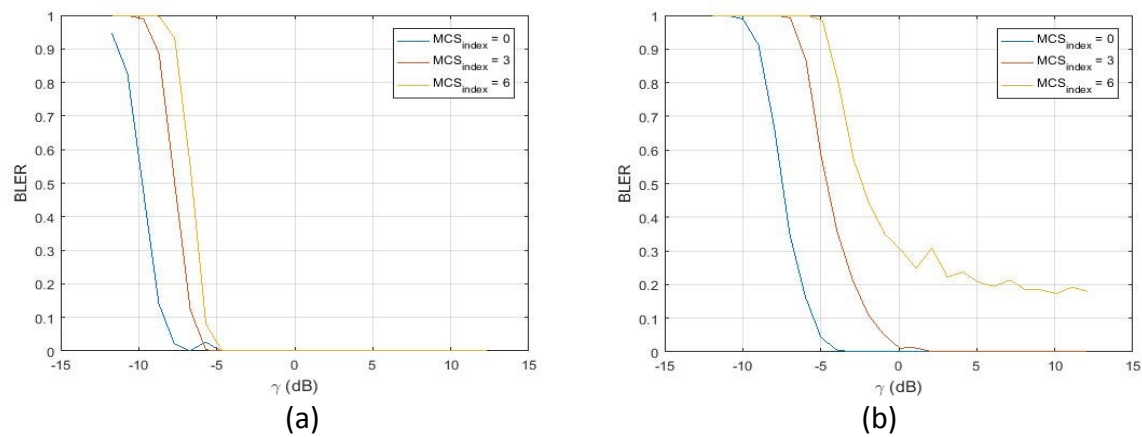


Figure 20. BLER ranging for 0 to 1. (a) SINR(γ) vs BLER plot for clock error of 1 Hz.
(b) SINR(γ) vs BLER plot for clock error of 12 Hz.

4.3 Analysis of Measurement Results

In chapter 4.2, the analysis shows that rise in clock errors impacts the overall radio link performance of the system. The analysis in this chapter focuses on relation between CFO and parameters such as retransmissions (R), SINR and BLER for different MCS Indexes. The retransmissions (R) is computed over 93,750 packets sent over radio link from UE to eNodeB for each MCS index [0, 3, 6]. Each packet is decoded successfully by eNodeB for certain number of retransmissions. The minimum retransmissions are 4 and maximum is 128. The average retransmissions (R) for MCS 0, 3 and 6 at various CFO is presented in Table 8.

Table 8. CFO, MCS and R (Avg.) at SINR \sim -5 dB

CFO	MCS Index	Average retransmissions (R)
95 Hz	0	15.41
	3	34.64
	6	55.89
480 Hz	0	30.29
	3	68.78
	6	93.87
805 Hz	0	48.33
	3	96.67
	6	113.62

In the above Table 8, Clock error of 1 Hz, 4 Hz, 7 Hz, 10 Hz and 12 Hz corresponds to CFO of 95 Hz, 289 Hz, 480 Hz, 677 Hz and 805 Hz. The clock error and corresponding CFO can be found out at Table 5. R is doubled when CFO is increased from 95 Hz to 480 Hz and tripled at 805 Hz for MCS index 0. The rise in R indicates compromised performance of radio link due to rise in clock error and CFO. The performance of the link gets worst for MCS index 6 as R rises to 114 out of 128 at CFO of 805 Hz. The values above are chosen for SINR of -5 dB as the range of SINR for measurement is -12 dB to 12 dB and -5 dB is a strong enough signal to receive packets correctly by eNodeB.

The plot (Fig. 21) is plotted for different clock errors that produces carrier frequency offset (CFO). The curved lines in the plot indicates Clock error of 1 Hz, 4 Hz, 7 Hz, 10 Hz and 12 Hz which corresponds to CFO of 95 Hz, 289 Hz, 480 Hz, 677 Hz and 805 Hz as seen in legend text. The clock error and corresponding CFO can be found out at Table 7. The interesting observation from the Figure is that after SINR of 5 dB, R is minimum and constant (i.e. 4 in the plot). This indicates that the signal is very strong at SINR of 5 dB and above. There is no loss of packets and the effects of CFO is minimum.

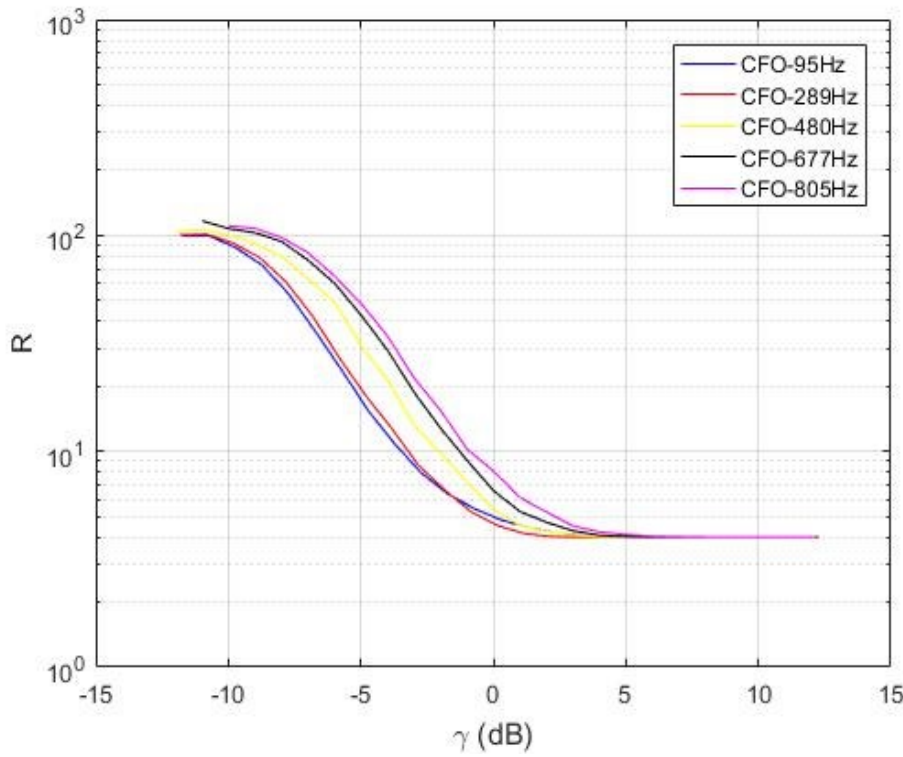


Figure 21. Plot showing SINR (γ) vs average retransmissions (R) for MCS 0.

The curves for higher CFO (677 Hz and 805 Hz) in Fig.22 do not reach minimum retransmissions ($R = 4$) even when the signal is strong (SINR of 5 dB and above). This could be mainly because higher MCS value has weaker protection of symbols against inter symbol interference (ISI). The curves at MCS 3 shows higher retransmissions compare to MCS 0 at a particular SINR values. At SINR of -5 dB, the curves with CFO 95 Hz, 480 Hz and 805 Hz has average retransmissions (R) of 34.64, 68.78 and 96.67 for MCS 3. The R is nearly doubled compared to MCS 0 ($R = 15.41, 30.29, 48.33$). The average retransmissions (R) is below 10 for all curves at around SINR of 5 dB for MCS 3 while R is below 10 at around SINR of 0 dB for MCS 0 for all curves. As compared to MCS index 0, SINR requirement is around 5 dB higher for MCS index 3 to reduce R below 10 for all curves.

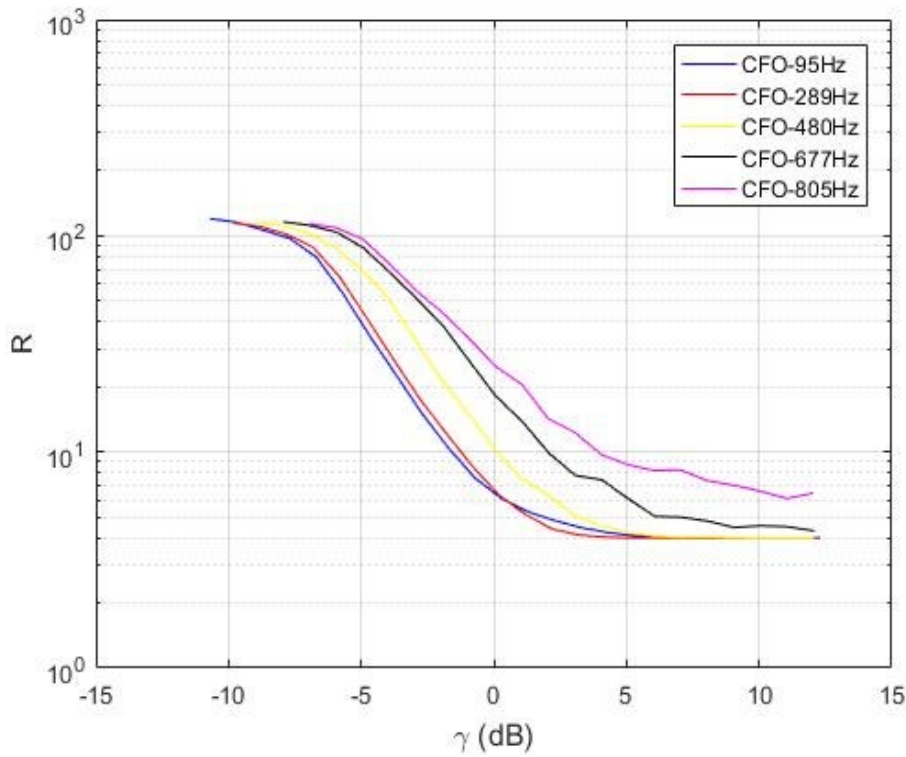


Figure 22. Plot showing SINR (γ) vs average retransmissions (R) for MCS 3.

The curves show even more average retransmissions (R) as the MCS Index is increased to 6 (Fig.23) for CFO of 677 Hz and 805 Hz. The R is quite high (i.e. ~ 10 for 677 Hz and ~ 15 for 805 Hz) at SINR of 10 dB while other curves has value of minimum retransmissions ($R = 4$). At SINR of -5 dB, the curves with CFO 95 Hz, 480 Hz and 805 Hz has average retransmissions (R) of 55.89, 93.87 and 113.62 for MCS 3. The R is nearly tripled if compared to MCS 0 ($R = 15.41, 30.29, 48.33$). The curves with CFO of 95 Hz, 289 Hz and 480 Hz attains the minimum retransmissions ($R=4$) around 8 dB but the curves with CFO of 677 Hz and 805 Hz never attains the minimum retransmissions. As compared to MCS index 0, SINR requirement is around 8-10 dB higher for MCS index 6 to reduce R below 10 for most of the curves.

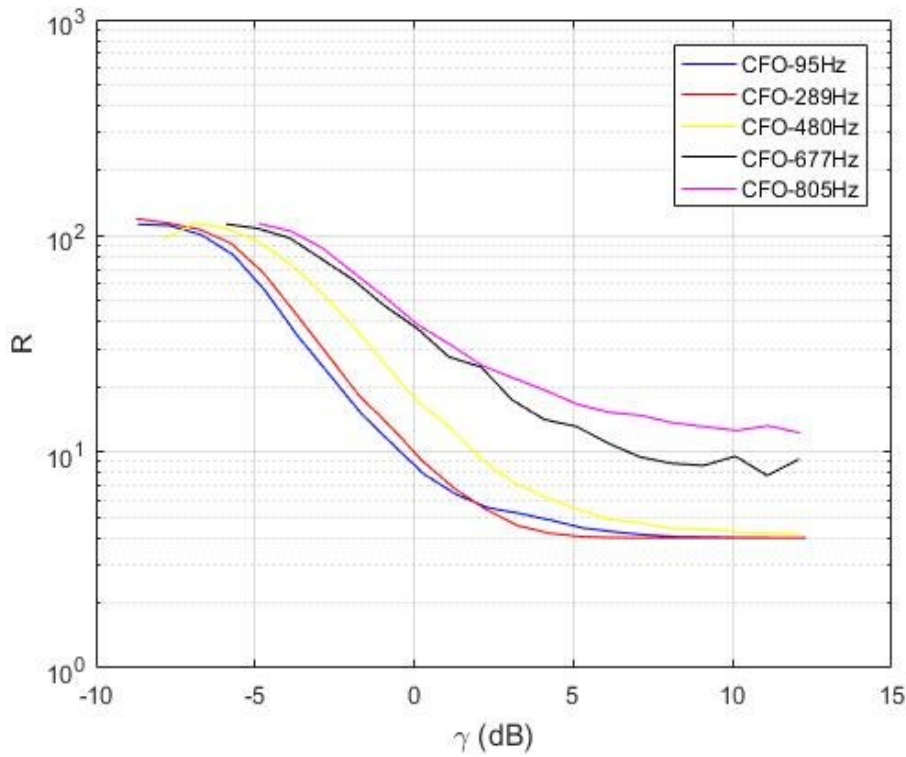


Figure 23. Plot showing SINR (γ) vs average retransmissions (R) for MCS 6.

The Table 9 below compares the CFO and BLER at various MCS Index showing interesting data from the measurement. All data are taken at SINR of -5 dB. There is significant rise in the value of BLER as CFO increases from 95 Hz to 805 Hz for MCS index of 6. The BLER reaches to near maximum (0.9842) for MCS index 6 at 805 Hz. However, the increase in BLER is very low for MCS index 0. This is because lower MCS index has better protection against ISI and are more robust than higher MCS indexes. The data from the table shows that there is heavy packet drops as CFO increases gradually. The radio link is hampered by higher CFO and clock errors resulting in significant drop of data packets in the link.

Table 9. CFO, MCS and BLER at SINR \sim -5 dB

CFO	MCS Index	BLER
95 Hz	0	0
	3	0.00026
	6	0.0029
480 Hz	0	0.0020
	3	0.1369
	6	0.4771
805 Hz	0	0.0434
	3	0.5761
	6	0.9842

The comparison between BLER and CFO is shown in the plots below. The plots SINR vs BLER are plotted corresponding to various CFO for MCS index 0 in Fig.24. There is increase in BLER as CFO rises until the signal level is good with high SINR. The BLER is below 0.1 (almost 0) for the curves with CFO 95 Hz and 289 Hz while the curves with CFO 480 Hz, 677 Hz and 805 Hz still have BLER value greater than 0.1 (around 0.3, 0.6, 0.7) for SINR of -8 dB. The BLER is almost 0 even for highest CFO of 805 Hz, when the signal is strong enough and has SINR of -5 dB. The BLER is 0 for all other curves when SINR rises to -5 dB and above.

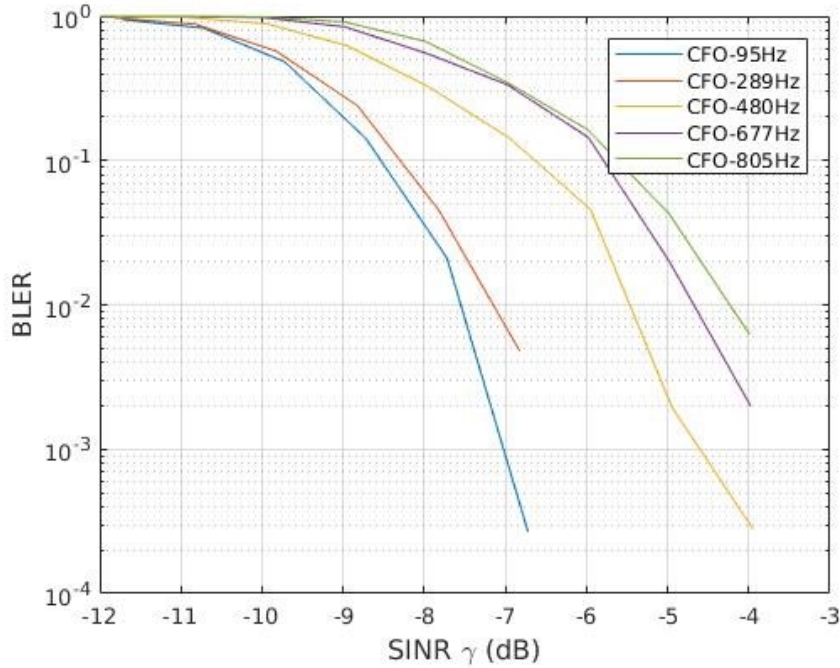


Figure 24. Plot showing SINR (γ) vs BLER for MCS 0.

The BLER value has a significant increase when MCS index is 3 and 6 for the same CFO and SINR value compared to MCS index 0. At SINR of -8 dB, all the curves with CFO of 95 Hz and above have high BLER value (above 0.6) reaching up to 1 for MCS index 3 as seen in Fig.25. Moreover, at SINR of -5 dB, curves with CFO 480 Hz, 677 Hz and 805 Hz have BLER of around 0.1, 0.3, 0.5 which is high as compared to MCS index 0. All the curves reach BLER value of 0 when the SINR is 0 dB and above for MCS 3. As compared to MCS index 0, SINR requirement is around 5 dB higher for MCS index 3 to reduce BLER value up to 0 for all curves.

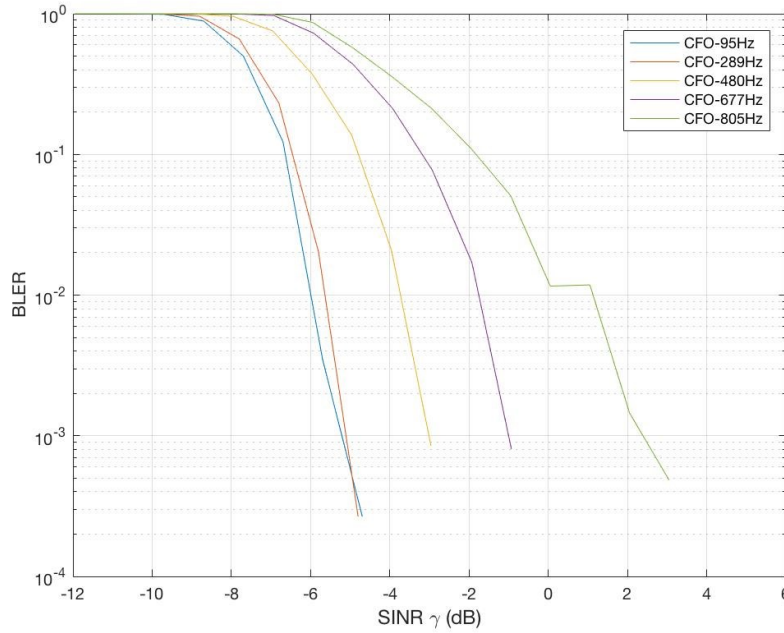


Figure 25. Plot showing SINR (γ) vs BLER for MCS 3.

The BLER value for MCS index 6 does not reach to 0 for all the curves even at the strongest signal of SINR 12 dB. The plot (Fig. 26) shows SINR vs BLER for MCS 6. The BLER is 1 for all the curves at SINR of -8 dB. If it is compared to MCS index 0, the curves with CFO 95 Hz and 289 Hz already had BLER value below 0.1 at SINR of -8 dB. Similarly, only curves with CFO of 95 Hz and 289 Hz have BLER value almost 0 at SINR of -5 dB while all other curves have significantly high BLER. The curve with CFO of 480 Hz attends BLER value lower than 0.1 around SINR of -3 dB while the curve with CFO of 677 Hz attends BLER value of 0.1 at SINR of 0 dB. The curves with CFO of 480 Hz and 677 Hz reaches to BLER value of almost 0 at SINR of around 1 dB and 4 dB but the curve with maximum CFO of 805 Hz has value above 0.1 dB for all SINR value. The curve with CFO of 805 Hz attains the minimum BLER value of 0.17 at the strongest signal level with SINR of 12 dB. The BLER is much higher for MCS index 6 as compared to MCS 0 for higher CFO because MCS index 6 has weaker protection against ISI and are more vulnerable to errors than lower MCS indexes.

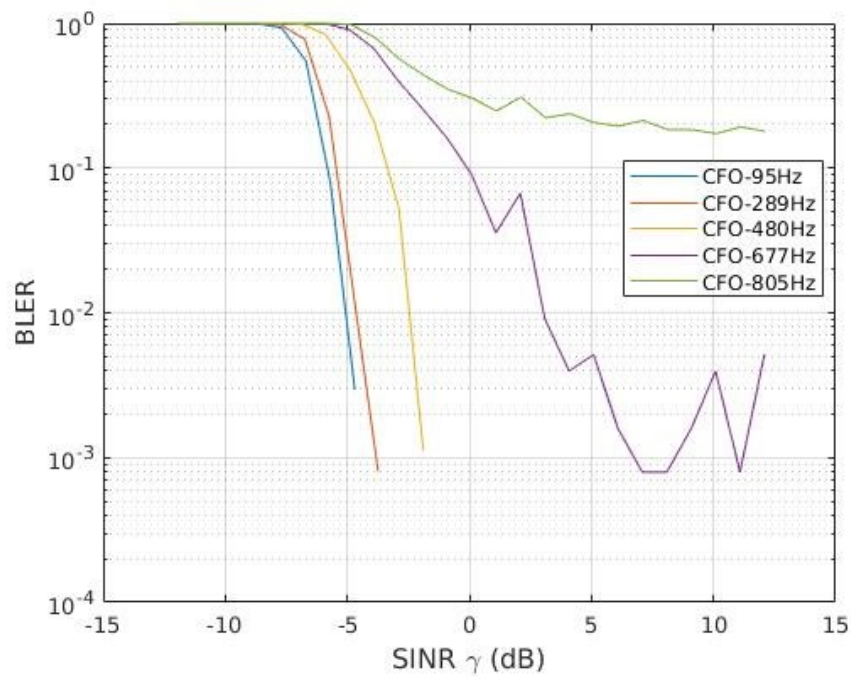


Figure 26. Plot showing SINR (γ) vs BLER for MCS 6.

5. Discussions of Results

This thesis work uses NB-IoT testbed to perform measurements to analyze the impact of clock error on the radio link performance of NB-IoT system. The system (NB-IoT testbed) has been implemented in the LTE stack on flexible software radios based C-RAN testbed. The system mostly focuses on implementation of lower layers therefore L1 and part of L2 and L3 protocol stack has been implemented. This implemented SDR can run any RAN technology on a commercially available personal computer. The test network enables to measure performance of NB-IoT system.

The measurements were taken for clock errors ranging from 1 Hz to 12 Hz. The analysis of measurement data showed that about 89% of the packets were successfully decoded by eNodeB for clock error of 1 Hz while only 49% packets were successfully decoded for clock error of 12 Hz. The above values are true for MCS 0. The general trend showed that MCS 3 and MCS 6 had decreased percentage of successfully decoded packets compared to MCS 0 for various clock errors.

Similarly, the average retransmissions R was high up to 99.4 out of 128 at SINR of -11.7 dB (weak signal) while R = 15.41 at SINR of -5 dB (good signal) and R (minimum) = 4 at SINR of 5 dB and above (strong signal) for clock error of 1 Hz. The values are true for MCS 0. The general trend showed that MCS 3 and MCS 6 had increased R compared to MCS 0 for all clock errors. The value of R reached up to 128 or more at SINR of -11.7 dB for MCS 3 and MCS 6.

Additionally, BLER showed significant increase as clock error rose from 1 Hz to 12 Hz. The BLER was high up to 0.9466 out of 1 at SINR of -11.7 dB (weak signal) while BLER = 0.026 at SINR of -5.5 dB (good signal) and BLER was 0 for higher SINR for clock error of 1 Hz and MCS 0. The general trend showed that MCS 3 and MCS 6 had increased BLER compared to MCS 0 for all clock errors. The BLER value was 0.17 even for the strongest signal at SINR of 12 dB for MCS 6 for clock error of 12 Hz.

The system (NB-IoT) used in this thesis has already been used for performance measurement. The measurement consisted of sending NB-PUSCH TB in two different scenarios: 1. static channel with Doppler shift of 0 Hz, 2. Fast fading channel with Doppler shift of 80 Hz. The former presents the best-case scenario while later presents the worst-case scenario that UE is expected to face. The measurement indicated that the coverage is limited by the coverage time of a fast fading channel. The measurement in static channel depicted that up to 20 dB uplink coverage gain could be achieved from 128 repetitions which would push the operating SNR below -20 dB for MCS 0. However, in fast fading channel, the SNR should be at least -12 dB implying that the coverage gain from repetitions is reduced by more than 10 dB as a result of short channel coherence time [8].

The NB-IoT system used in this thesis work is a practical system which make use of efficient and reliable devices. The USRP devices that acts as UE and eNodeB consists of TCXO which

produces precise frequencies with frequency accuracy of 2.5 ppm. Similarly, signal generators that are used to insert reference clock signal of 10 MHz to the USRP's provides precision of 0.01 ppm. With such precise devices, the error generated is much less. Without any clock error introduces in the system, the CFO generated was $33 \text{ Hz} / 0.051 \text{ ppm}$ for 640 MHz which is small. But low-cost devices that NB-IoT intends to use as UE are equipped with low cost crystal oscillators that can have an initial carrier frequency offset (CFO) of several PPM. With such large CFO, the primary problem could be synchronization between UE and BS which will eventually lead to higher packet drops. Moreover, NB-IoT intends to provide extended coverage for UE deployed in environments in high penetration loss, e.g., under basement of a building. The extended coverage is possible with higher retransmissions of signal. With such high CFO and synchronization issues, the retransmissions of signal by UE would rise significantly. In addition, the overall performance of the system could be compromised.

There are several companies and vendors that are producing commercial chipsets for NB-IoT technology. Some of the vendors are u-blox, Quectel, Huawei, Digi and AT&T. The chipsets are mainly designed for NB-IoT and LTE-M technologies (3GPP Release 13) and at different LTE bands. The vendors are on their way to commercialize them soon. The vendors promise to provide compact size, longer battery life and reduced-cost of devices (but still higher than the target of 5€). These low-cost devices will have cheap and poor performance oscillators that would produce large clock offsets and CFO. Despite of this large CFO, UE (devices) should be able to perform its operations (synchronization and packet transmissions) at very low SINR.

The chipsets are believed to produce CFO of several PPM as large as up to 20 ppm. The UE has to compensate for this high CFO during synchronization with BS. Moreover, NB-IoT system already has a raster offset of up to 7.5 KHz. Therefore, UE has to correct / compensate for both the offsets (raster and CFO) during synchronization. The same NB-IoT testbed (used in this thesis work) can be used to find out the performance of chipsets when available. It would be interesting to observe how the chipsets perform under conditions where the signal level is low and enhanced coverage is required. Some curious questions in regard to chipsets would be How much CFO is generated by the chipset and what is its effect on synchronization process? How many packet retransmissions are required when signal is weak for both DL and UL? What modifications are needed in the specifications of chipsets to make it work better with NB-IoT system?

6. Conclusion

The thesis work uses NB-IoT testbed implemented on a flexible SDR based C-RAN. The thesis briefly describes the targets of NB-IoT such as low cost, low power consumption, delay non-sensitive, massive support for large number of devices and easy deployment. The physical channels and modulation access techniques (OFDMA and SC-FDMA) associated with the technology has been discussed in brief. The study of performance issues on NB-IoT such as long battery life, extended coverage, latency is also summarized in this thesis. Moreover, background of the problems associated with NB-IoT such as clock synchronization and CFO are briefly introduced in chapter 2.

The task of this thesis is to study the impact of clock error in the radio link of the NB-IoT testbed. The measurement setup is designed to capture data from uplink transmissions and analyze them. The NB-IoT testbed uses uplink and downlink frequency band of 635 MHz and 640 MHz. The USRP A (eNodeB) and USRP B (UE) are fed with external clock signals to manually input clock error. The clock signals fed to USRP's are standard 10 MHz signal. The clock error ranges from 1 Hz to 12 Hz. The measurements are taken for clock error of 1 Hz to 12 Hz and data are analyzed to observe the radio link performance at different clock errors. The parameters such as SINR, R and BLER are considered in this thesis work.

Around 89% of packets are correctly decoded for MCS 0 when clock error is minimum (1 Hz) whereas only 49% of packets are correctly decoded when clock error rises to 12 Hz. The packet drops are higher for MCS 3 and MCS 6 at all SINR values as compared to MCS 0. The retransmissions R has minimum value of 4 when SINR is high but R increases significantly when SINR is low. The minimum average retransmissions R is found to be 15.41 for MCS 0 when CFO is 95 Hz at SINR of -5 dB. The maximum average retransmissions R is found up to 114 for MCS 6 when CFO is 805 Hz at SINR of -5 dB. Similarly, BLER is 0 (i.e. minimum) for MCS 0 when CFO is 95 Hz at SINR of -5 dB. The maximum BLER is noted to be 0.9842 for MCS 6 when CFO is 805 Hz at SINR of -5 dB.

The relation between parameters SINR and R has been observed for clock error range of 1 Hz to 12 Hz and MCS index (0, 3 and 6). The value of R rises from 4 to 128 at SINR of -12 dB to 12 dB for different MCS index and clock errors. The R is found to be minimum and constant at SINR of 5 dB and above for MCS 0 indicating that there is no packet loss and effect of CFO is minimum. Similarly, the relation between parameters SINR and BLER has been observed for clock error range of 1 Hz to 12 Hz and MCS index (0, 3 and 6). BLER is almost 0 even for maximum CFO of 805 Hz for MCS 0, when the signal is strong enough and has SINR value of -5 dB. BLER is high and reaches up to 1 when SINR is low around -8 dB and less for all CFO values.

The thesis work and result from the analysis suggests that NB-IoT is vulnerable to synchronization issues and the radio link performance degrades as clock error increases. The measurements show that when clock error increases by 1 Hz, CFO of the network increases by several Hz. When CFO rises to 100's of Hz, the synchronization between UE and eNodeB

becomes difficult and many transmitted data packets are dropped by eNodeB. Since data rate and latency requirements are relaxed for the NB-IoT, the robustness of the network can be increased using lower MCS index.

The further study and analysis could include the measurement of downlink transmission of signal when clock error is introduced in the system. The same measurement setup can be used to collect data and similar analysis can be performed to figure out the impact of clock error in the radio link performance. The measurements can be performed over the air instead of cable connections between USRP's to understand interference and degradation of signals in the air. The measurement in this thesis work is conducted for a stationary UE. Therefore, further study could also include moving or mobile UE and observe the impact of Doppler's shift in the radio link performance. Moreover, it could be interesting to investigate fading effects.

References

- [1] Nokia white paper, “LTE evolution for IoT connectivity”, [Online]. Available: <http://resources.alcatel-lucent.com/asset/200178> [Accessed 15 nov., 2017].
- [2] Ericsson white paper, “Cellular Networks for Massive IoT”, [Online]. Available: http://www.ericsson.com/res/docs/whitepapers/wp_iot.pdf [Accessed 10 oct., 2017].
- [3] Huawei white paper, “NB-IOT-Enabling New Business Opportunities”, [Online]. Available: http://www.huawei.com/minisite/iot/img/nb_iot_whitepaper_en.pdf [Accessed 17 oct., 2017].
- [4] Rohde&Schwarz white paper, “Narrowband Internet of Things”, [Online]. Available: https://cdn.rohde-schwarz.com/pws/dl_downloads/dl_application/application_notes/1ma266/1MA266_0e_NB_IoT.pdf [Accessed 10 mar., 2017].
- [5] Y. Wang, X. Lin, A. Adhikary, A. Grovlen, Y. Sui, Y. Blankenship, J. Bergman and H. Razaghi, "A Primer on 3GPP Narrowband Internet of Things", IEEE Communications Magazine, vol. 55, no. 3, pp. 117-123, 2017.
- [6] R. Ratasuk, N. Mangalvedhe, Y. Zhang, M. Robert and J. Koskinen, "Overview of narrowband IoT in LTE Rel-13", 2016 IEEE Conference on Standards for Communications and Networking (CSCN), 2016.
- [7] R. Ratasuk, N. Mangalvedhe, Y. Zhang, M. Robert and J. Koskinen, “NB-IoT System for M2M Communication” 2016 IEEE Workshop on Device to Device communications for 5G NETWORKS (WD5G), 2016.
- [8] Y. D. Beyene, R. Jäntti, O. Tirkkonen, K. Ruttik, S. Iraj, A. Larmo, T. Tirronen and J. Torsner, “NB-IoT Technology Overview and Experience from Cloud-RAN Implementation”, 2016.
- [9] Freescale Semiconductor white paper, “Overview of the 3GPP Long Term Evolution Physical Layer”, [Online]. Available: <http://www.nxp.com/assets/documents/data/en/whitepapers/3GPPEVOLUTIONWP.pdf> [Accessed 21 may., 2017].
- [10] ETSI TS 136 213 V8.8.0 Technical Specification, “LTE; Evolved Universal Terrestrial Radio Access (E-UTRA); Physical layer procedures (3GPP TS 36.213 version 8.8.0 Release 8), 2009-10.
- [11] Symmetricom white paper, “Timing and Synchronization for LTE-TDD and LTE-Advanced Mobile Networks”, [Online]. Available: <https://www.aventasinco.com/whitepapers/WP-Timing-Sync-LTE-SEC.pdf> [Accessed 14 july, 2017].

- [12] Ericsson Technology Paper, "Network Synchronization", [Online]. Available: <http://archive.ericsson.net/service/internet/picov/get?DocNo=5/28701-FGB101686&Lang=EN&HighestFree=Y> [Accessed 16 aug., 2017].
- [13] A. van Zelst and T. Schenk, "Implementation of a MIMO OFDM-Based Wireless LAN System", IEEE Transactions on Signal Processing, vol. 52, no. 2, pp. 483-494, 2004.
- [14] En Zhou, Xing Zhang, Hui Zhao and Wenbo Wang, "Synchronization algorithms for MIMO OFDM systems", IEEE Wireless Communications and Networking Conference, 2005.
- [15] T. Chiueh, P. Tsai, Lai. I-Wei. And T. Chiueh, Baseband receiver design for wireless MIMO-OFDM communications, 2nd edition, 2012.
- [16] "USRP N200 Software Defined Radio (SDR) - Ettus Research", Ettus.com, [Online]. Available: <https://www.ettus.com/product/details/UN200-KIT> [Accessed 10 jan., 2018].
- [17] "R&S®RSC Step Attenuator - Overview", Rohde-schwarz.com, [Online]. Available: https://www.rohde-schwarz.com/us/product/rsc-productstartpage_63493-11395.html [Accessed 17 aug., 2017].
- [18] "R&S®SMBV100A Vector Signal Generator - Overview", Rohde-schwarz.com, [Online]. Available: https://www.rohde-schwarz.com/us/product/smbv100a-productstartpage_63493-10220.html [Accessed 17 aug., 2017].
- [19] "Spectrum Analyzers | Tektronix", Tek.com, [Online]. Available: <http://www.tek.com/datasheet/rsa6000-series> [Accessed 17 aug., 2017].
- [20] "MDO3000 Mixed Domain Oscilloscope | Tektronix", Tek.com, [Online]. Available: <http://www.tek.com/oscilloscope/mdo3000-mixed-domain-oscilloscope> [Accessed 17 aug., 2017].
- [21] "Rohde & Schwarz Time Synchronous Signals with Multiple R&S®SMBV100A Vector Signal Generators", [Online]. Available: https://cdn.rohde-schwarz.com/pws/dl_downloads/dl_application/application_notes/1gp84/1GP84_1E_Synchronous_Signals_with_SMBVs.pdf [Accessed 17 aug., 2017].
- [22] S. Landström, J. Bergström, E. Westerberg, D. Hammarwall, Ericsson Technology Review, "NB-IOT: A SUSTAINABLE TECHNOLOGY FOR CONNECTING BILLIONS OF DEVICES", 2016.
- [23] Samsung Networks white paper, "Internet of Things", [Online]. Available: <http://www.samsung.com/global/business-images/insights/2016/IoT-Whitepaper-0.pdf> [Accessed 17 july, 2017].

- [24] P. Manhas, S. Thakral, Dr. A. Arora, “Synchronization Issues in Wireless OFDM Systems: A Review”, International Journal of Engineering Research & Technology (IJERT), ISSN: 2278-0181, Vol. 3 Issue 3, March - 2014.
- [25] N. Mangalvedhe, R. Ratasuk, and A. Ghosh, “NB-IoT Deployment Study for Low Power Wide Area Cellular IoT”, IEEE 27th Annual International Symposium on Personal, Indoor, and Mobile Radio Communications (PIMRC) - Workshop: From M2M Communications to Internet of Things, 2016.
- [26] A. Lometti, G. Cazzaniga, S. Frigerio, L. Ronchetti, “Synchronization Techniques in Back-hauling Networks”, International Conference on Optical Transparent Network (ICTON), 2013.
- [27] R. Prasad, “OFDM for Wireless Communications Systems”, 2004.
- [28] “USRP N200 Datasheet”, Ettus.com, [online]. Available: https://www.ettus.com/content/files/07495_Ettus_N200-210_DS_Flyer_HR.pdf [Accessed 12 dec., 2017].
- [29] “Installing the Ettus Research GPSDO Kit for USRP N200 series and E100 Series”, Ettus.com, [online]. Available: https://www.ettus.com/content/files/gpsdo-kit_2.pdf [Accessed 12 dec., 2017].
- [30] “R&S®SMBV100A Signal Generator- Data Sheet”, [online]. Available: https://cdn.rohde-schwarz.com/pws/dl_downloads/dl_common_library/dl_brochures_and_datasheets/pdf_1/SMA100A_dat-sw_en_5213-6412-22_v0700.pdf [Accessed 12 dec., 2017].

A Appendix: Modulation TBS index for PDSCH & PUSCH

Table 10. Modulation index and TBS index for PDSCH [10]

MCS Index I_{MCS}	Modulation Order Q_M	TBS Index I_{TBS}
0	2	0
1	2	1
2	2	2
3	2	3
4	2	4
5	2	5
6	2	6
7	2	7
8	2	8
9	2	9
10	4	9
11	4	10
12	4	11
13	4	12
14	4	13
15	4	14
16	4	15
17	6	15
18	6	16
19	6	17
20	6	18
21	6	19
22	6	20
23	6	21
24	6	22
25	6	23
26	6	24
27	6	25
28	6	26
29	2	reserved
30	4	
31	6	

Table 11. Modulation, TBS index and redundancy version for PUSCH [10]

MCS Index I_{MCS}	Modulation Order Q_M	TBS Index I_{TBS}	Redundancy version rv_{idx}
0	2	0	
1	2	1	0
2	2	2	0
3	2	3	0
4	2	4	0
5	2	5	0
6	2	6	0
7	2	7	0
8	2	8	0
9	2	9	0
10	4	10	0
11	4	10	0
12	4	11	0
13	4	12	0
14	4	13	0
15	4	14	0
16	4	15	0
17	6	16	0
18	6	17	0
19	6	18	0
20	6	19	0
21	6	19	0
22	6	20	0
23	6	21	0
24	6	22	0
25	6	23	0
26	6	24	0
27	6	25	0
28	6	26	0
29	2	reserved	1
30	4		2
31	6		3

B Appendix: Specifications of N2x0, Internal GPSDO and Rhode and Schwartz Signal Generator

Table 12. Specifications of USRP N2x0 from Ettus Research [28]

Spec	Typ.	Unit	Spec	Typ.	Unit
POWER			RF PERFORMANCE (w/ WBX)		
DC Input	6	V	SSB/LO Suppression	35/50	dBc
Current Consumption	1.3	A	Phase Noise (1.8 Ghz)		
w/ WBX Daughterboard	2.3	A	10 kHz	-80	dBc/Hz
CONVERSION PERFORMANCE AND CLOCKS			100 kHz	-100	dBc/Hz
ADC Sample Rate	100	MS/s	1 MHz	-137	dBc/Hz
ADC Resolution	14	bits	Power Output	15	dBm
ADC Wideband SFDR	88	dBc	IIP3	0	dBm
DAC Sample Rate	400	MS/s	Receive Noise Figure	5	dB
DAC Resolution	16	bits	PHYSICAL		
DAC Wideband SFDR	80	dBc	Operating Temperature	0 to 55°	C
Host Sample Rate (8b/16b)	50/25	MS/s	Dimensions (l x w x h)	22x16x5	cm
Frequency Accuracy	2.5	ppm	Weight	1.2	kg
w/ GPSDO Reference	0.01	ppm			

Table 13. Specifications of internal GPSDO kit from Ettus Research [29]

Module Specifications

1 PPS Accuracy	$\pm 50\text{ns}$ to UTC RMS (1-Sigma) GPS Locked
Holdover Stability	$< \pm 11\mu\text{s}$ over 3 hour period at +25C
1 PPS Output (OCXO Flywheel Generated)	3.3VDC CMOS
RS-232 Control	NMEA & SCPI-99 Control Commands, Integrated into UHD
GPS Frequency	L1, C/A 1574MHz
GPS Antenna	Active (3V compatible) or Passive
GPS Receiver	50 Channels, Mobile, WAAS, EGNOS, MSAS capable
Sensitivity	Acquisition -144dBm, Tracking -160dBm
TTF	Cold Start: <45 sec, Warm Start: 1 sec, Hot Start: 1 sec
ADEV	1E-11 at 1s
Warm Up Time / Stabilization Time	<5 min at +25C to 1E-08 Accuracy
Supply Voltage (Vdd)	6VDC
Power Consumption	<1.8W Max, 1.35W Typical
Operating Temperature	0C to +60C
Storage Temperature	-45C to 85C

Oscillator Specifications

Frequency Output	10MHz	
10MHz Retrace	$\pm 2\text{E}-08$ after 1 hour at 25C	
Frequency Stability Over Temperature (Unlock Condition)	$\pm 2.5\text{E}-08$	
Warm Up Time	< 1 min at +25C	
Phase Noise at 10MHz	1Hz	-80dBc/Hz
	10Hz	-110dBc/Hz
	100Hz	-135dBc/Hz
	1kHz	-145dBc/Hz
	10kHz	<-145dBc/Hz

Table 14. Specifications of Signal Generator from Rhode and Schwartz [30]

Reference frequency

Frequency error	at time of calibration in production	$< 1 \times 10^{-8}$
	with R&S®SMA-B22 option	$< 5 \times 10^{-9}$
Aging	after 10 days of uninterrupted operation	$\leq 1 \times 10^{-9}/\text{day}, \leq 1 \times 10^{-7}/\text{year}$
	with R&S®SMA-B22 option	$\leq 5 \times 10^{-10}/\text{day}, \leq 3 \times 10^{-8}/\text{year}$
Maximum temperature effect	in temperature range 0 °C to +50 °C	$\pm 6 \times 10^{-8}$
	with R&S®SMA-B22 option	$\pm 6 \times 10^{-9}$
Warm-up time	to nominal thermostat temperature	$\leq 10 \text{ min}$
Reference frequency output		
Connector type	REF OUT on rear panel	BNC female
Output frequency	sine wave	
	instrument set to internal reference	10 MHz
	instrument set to external reference	applied external reference frequency
Output level		2 dBm to 8 dBm
		5 dBm to 7 dBm (typ.)
Source impedance		50 Ω (nom.)
Reference frequency input		
Connector type	REF IN on rear panel	BNC female
Input frequency		5 MHz, 10 MHz or 13 MHz
Min. frequency locking range		$\pm 3 \times 10^{-6}$
	with R&S®SMA-B22 option	$\pm 1.5 \times 10^{-7}$
Input level range	level limits	$\geq -6 \text{ dBm}, \leq 19 \text{ dBm}$
	recommended input level	0 dBm to 19 dBm
Input impedance		50 Ω (nom.)
Input for electronic tuning of internal reference frequency		
Connector type	EXT TUNE on rear panel	BNC female
Sensitivity		$0.5 \times 10^{-8}/\text{V}$ to $3 \times 10^{-8}/\text{V}$
		$1 \times 10^{-8}/\text{V}$ to $2 \times 10^{-8}/\text{V}$ (typ.)
	with R&S®SMA-B22 option	$5 \times 10^{-9}/\text{V}$ to $2 \times 10^{-8}/\text{V}$
		$8 \times 10^{-9}/\text{V}$ to $9.5 \times 10^{-9}/\text{V}$ (typ.)
Input voltage		-10 V to +10 V
Input impedance		10 k Ω (nom.)
	with R&S®SMA-B22 option	5 k Ω (nom.)

C Appendix: Brief Introduction of the devices used for thesis work measurement

A brief introduction about the devices is below.

- USRP N200 series is a software defined radio designed and produced by Ettus research that provides high performance, high bandwidth and high dynamic range. It operates from DC to 6 GHz. Data streaming and programming of device can be done through gigabit Ethernet port. It provides sampling rate up to 50 MS/s to and from host applications. [16]
- Step attenuator used in the measurement is a switchable and mechanical step attenuator designed and produced by Rohde and Schwarz. It operates on frequency range from Dc to 6 GHz. The device provides maximum attenuation of 139 dB and minimum step size of 0.1 dB and it can be remotely controlled. [17]
- Signal Generators used in the measurement is a Rohde and Schwarz SMBV100A vector signal generator. It has excellent RF performance and high output level and short setting time. It generates number of digital standard signals when equipped with an internal baseband generator such as (LTE, LTE-advanced and IEEE 802). The device frequency ranges from 9 KHz to 6 GHz and it's level ranges from -145 dBm to +18 dBm. [18]
- Real Time Signal generator is a high-performance spectrum analyzer and its frequency range from 9 KHz to 14 GHz. The device provides DPX spectrum processing which provides intuitive (easy and simple) understanding of Time-varying RF. It has multiple window spectrum view [DPX, spectrum, spectrogram]. The device has lots of functions to for analysis of signals. [19]
- Digital Oscilloscope is designed and produced by Tektronix. It has analog bandwidth of 500 MHz and sample rate 2.5 Gs/s. It provides multiple signal input and easy analysis of signals. The equipment has multiple functions such as spectrum analysis, function generator and many more. It captures analog, digital and RF signals with one scope. [20]
- The host server (Personal Computer) is a high-performance desktop with multi Ethernet ports and good processor.

D Appendix: IP addresses of the USRPs and devices used in the measurement setup

IP Address	Device	Name at the network
192.168.10.2	USRP A (eNodeB)	etho 0
192.168.20.2	USRP B (UE)	etho 1
192.168.48.30	Step Attenuator	etho 4

E Appendix: Picture of the overall Measurement Setup

